CR-166226
(R McLaughlin)

STRAY LIGHT IN THE

INFRARED ASTRONOMICAL SATELLITE (IRAS)

Breault Research Organization, Inc.

1161 El Dorado Place, Suite 340

Tucson, Arizona 85715

Steven R. Lange

Robert P. Breault

Prepared under Purchase Order No. A-69334B by
Breault Research Organization, Inc.
for
Ames Research Center
National Aeronautics and Space Administration
Moffett Field, California

January 1980

Table of Contents

Table of Contents (cont.)

Figures

Tables

Tables (cont.)

1.0 INTRODUCTION

This report documents the stray light analysis of the Infrared Astronomical Satellite including the propagation of scattered light, diffracted then scattered radiation, and thermally emitted radiation. The analysis was performed using Version 6 of the APART program and the PADE program for the diffraction.

An analysis of the flight system and the OSS was performed by the Breault Research Organization during the summer of 1978 which included the scattering and diffraction analysis. The results were presented in a report titled "Infrared Astronomical Satellite (IRAS); Analysis of the Transmittance of Off-Axis Energy due to Scattering and Diffraction" and dated June 30, 1978. The flight system has changed since that analysis, and the effect of those changes as well as better knowledge of the scattering properties of the optical elements have been obtained and will be commented on at the end of the report.

Many details of the mathematical modeling of IRAS and the analysis technique are the same as was previously done; thus this report will reference the first report when pertinent.

Tasks

The tasks to be accomplished during this contract are summarized from the statement of work below:

1. Update model to flight system of IRAS

1.1 Transmit list of assumptions in analysis

1.2 Calculate OAR for each spectral band for source angles: 1, 2, 3, 5, 10, 15, 20, 25, 30, 35, 40, 45, 55, 60, 75, 88, 110, 120, 130, 150. Both for 180^{o} azimuth and -90^{0} azimuth.

1.3 Calculate irradiance due to thermal emission for each IR band.

1.4 Calculate irradiance due to diffraction from the front aperture for the angles and azimuths of 1.2.

1.5 Do integration of earth's radiation in each IR band for angles: 88, 110, 120, 130, 150.

2.0 Document results of the analysis.

3.0 Review results with NASA/ARC.

For comparison, the previous analysis considered 9 angles of 5, 10, 17, 24, 30, 60, 88, 98, and 108 degrees in the 180^{o} azimuth only.

Items not considered

A number of items were not included in this contract although they were recommended:

1) Pure Diffraction: This was done in the previous analysis, although only for the aforementioned angles. It is difficult to include the previous results because of the differance in the angles sampled. Therefore, no addition of the former pure diffraction analysis will take place. The former plots are included in the A(θ) plots of this report for referance. Referances in this report to the sum of scatter and diffraction means the summation of the results of doing tasks 1.2 and 1.4.

2) Diffraction then scatter (complete): Presently this task is being done only for diffraction off the front-aperture ring. All of the other vane tips that are illuminated will also contribute energy via this propagation method so the total contribution from this mechanism will be difficult to predict. Only the front-aperture ring contribution will be presented in the results, but the omission of the other vane tips' contribution should be noted whenever this

mechanism is important.

3) Thermal emission from interior of IRAS: The only object we are considering as a thermal emitter is the sunshade with a temperature of 80°K and an emissivity of 0.02. Although the remaining interior is at a much lower temperature, it does have an emissivity of about 0.99 and a considerably higher configuration factor for transmittance of emitted radiation to the detector, which may compensate such that the interior may be as important as the sunshade in the thermal emission contribution.

4) Thermal emission and then diffraction: Presently we are considering the thermal emission from the sunshade scattering off the end of the main tube to a critical object before the energy can reach the image. Another propagation path is one in which the thermally emitted radiation diffracts off the vane tips to a critical object. At longer wavelengths the diffraction path may be important and its effect should be estimated.

Requirements

The telescope stray light rejection requirements are expressed in terms of $A(\theta)$ as defined by;

$$A(\theta) - \frac{1}{\Omega} \frac{P(\theta)}{P(0)} \text{ str.}^{-1}$$

A detailed discussion of this specification is presented in the 1978 report. The spectral bands and the required $A(\theta)$ are presented in Table 1 as reproduced from Specfication 2-26412.

Table 1. Required $A(\theta)$ sr^{-1}

	Spectral Band (μm)				
θ	0.4 - 0.9	8 - 15	15 - 30	48 - 81	87 - 118
5°	1×10	7×10^{0}	3×10^{-1}	4×10^{-2}	2×10^{-2}
24°	3×10^{-1}	1×10^{-5}	8×10^{-6}	4×10^{-6}	5×10^{-6}
60°	3×10^{-7}	5×10^{-8}	1×10^{-7}	2×10^{-7}	1×10^{-7}
88°	1×10^{-7}	2×10^{-8}	9×10^{-9}	4×10^{-9}	4×10^{-9}

Changes from Previous Analysis

A number of changes have been made in the telescope since the first analysis with the one having the most significant effect on the stray light being the new secondary baffle. The old secondary baffle consisted of an unvaned cone extending out from the secondary mirror. The new cone has been broken up into a series of steps which follow a similar slope. The steps break up the high forward scattering path present in the previous design. This change added considerable complexity to the analysis because now 20 objects were required to characterize the baffle, while only two were used before.

The second major change was in the shape of the tip of the inner primary baffle. Discontinuous cones are now used, further increasing the complexity of the modeling. This baffle was not a major contributor in the previous analysis except for the visible detectors which receive direct forward scattering from the inside of the cone.

A slight change was made around the primary aperture. Since these areas are not seen by an on-axis detector, the modification produced no significant change in the scattering.

A better modeling of the sunshade and front aperture plate was provided because of the availability of detailed and well dimensioned drawings of these components that were not available to us for the first analysis. This, as well as a better understanding of the diffraction rejection design, will produce a superior analysis of the system at the larger source angles.

The damaged area on the primary mirror was also included in this analysis. At the time the damage occurred, we did an analysis

for Kitt Peak National Observatories based upon an assumed BRDF for the area, which indicated the damaged area could be a major contributor at a range of angles from 30° to 60°; but its effect was probably no more than to double the radiation reaching the image. This analysis used the measured BRDF of the damaged area to determine the scattering model.

The BRDF of the primary mirror has been measured in both the visible and 10.6μm infrared. The data for the BRDF in the visible was used for the whole mirror with the damaged area not considered since the visible measurement included its effect. For the 10.6μm case, the BRDF of the mirror was used as well as the BRDF of the damaged area. When wavelength scaling was done for the three longer wavelengths, the two BRDFs were scaled separately and the total power adjusted accordingly.

2.0 SYSTEM MODELING

The accuracy to which the APART program can be used to predict stray light performance is dependent upon the modeling of the optical system's geometry as well as the accuracy of the measurements of the scattering properties of the surfaces in the system. A complete description of the assumptions used in the geometry, orientation, and BRDF models was supplied to NASA/ARC in a report dated November 22, 1979 and is reproduced in this report as Appendix A. Details of the system modeling will be found in Appendix A, while a summary of the pertinent details will be discussed in this section.

Geometrical input

A computer-produced plot of the IRAS system as modeled into APART is shown in Figure 1. Details of the modeling of the secondary baffle and primary cone baffle are shown in Figures 2 and 3 respectively. Objects 5 and 6 represent the vaned parts of the main tube with a cylinder located at the locus of the vane tips. Discussion of the diffraction edges of the sunshade and front aperture will be presented in the diffraction section later in this report. In all, 50 objects (cones, disks, struts, etc.) were used to describe the geometry of IRAS.

An important parameter in the efficiency of a stray light optical design is how many objects can be seen from the detector plane (critical objects) and what are the scattering properties of these objects. Ideally, it would be desirable for the detector to see just low-scatter optical elements and the backsides of field stops and Lyot stops. However, with the IRAS design a number of "critical" objects are seen that are high-scattering black surfaces (e.g. secondary baffle and aperture stop). A list of the critical objects and the space they are seen in is presented in Table 2. Some critical objects are not listed (e.g. the baffle cone directly in front of the detector plane) because they do not receive direct radiation at any of the point source angles considered.

Field masks

A discussion of the effect of the field masks and field lenses on the stray light in IRAS and their modeling by APART was reported on in the 1978 report. Briefly, the combination of the two produce an elliptical cone directed along the chief ray toward the exit pupil which

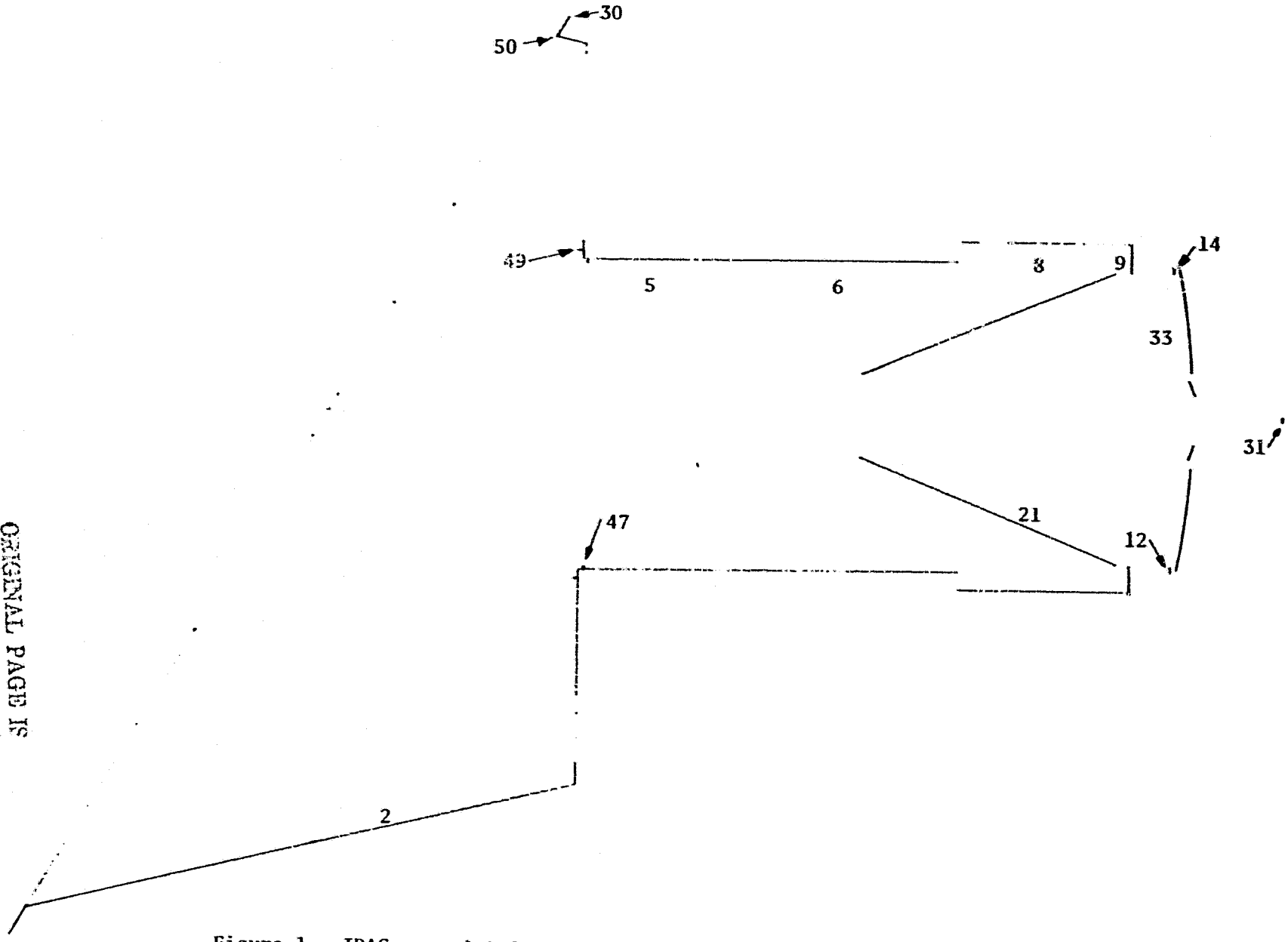

Figure 1. IRAS as modeled into APART.

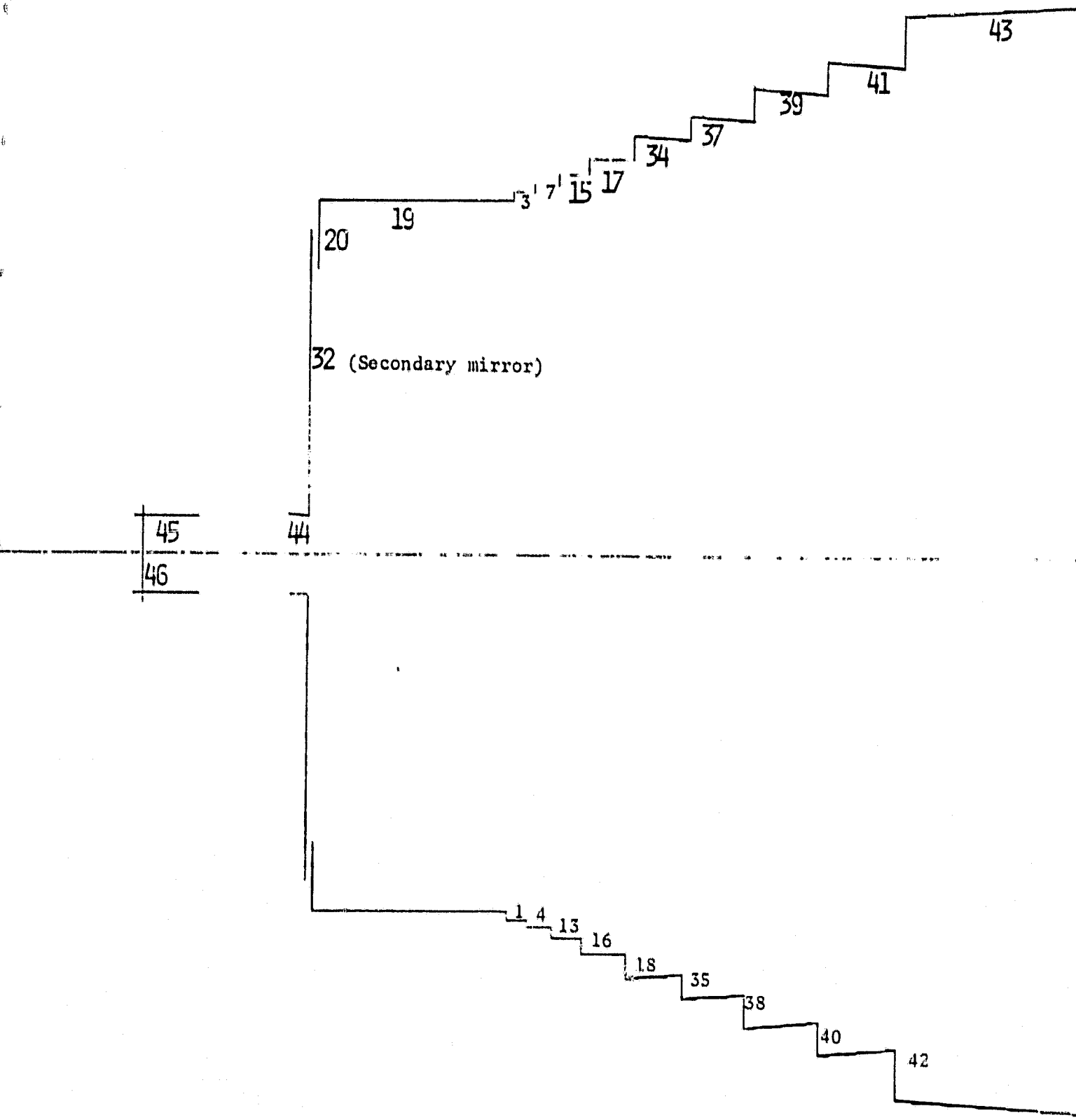

Figure 2. Details of the secondary baffle.

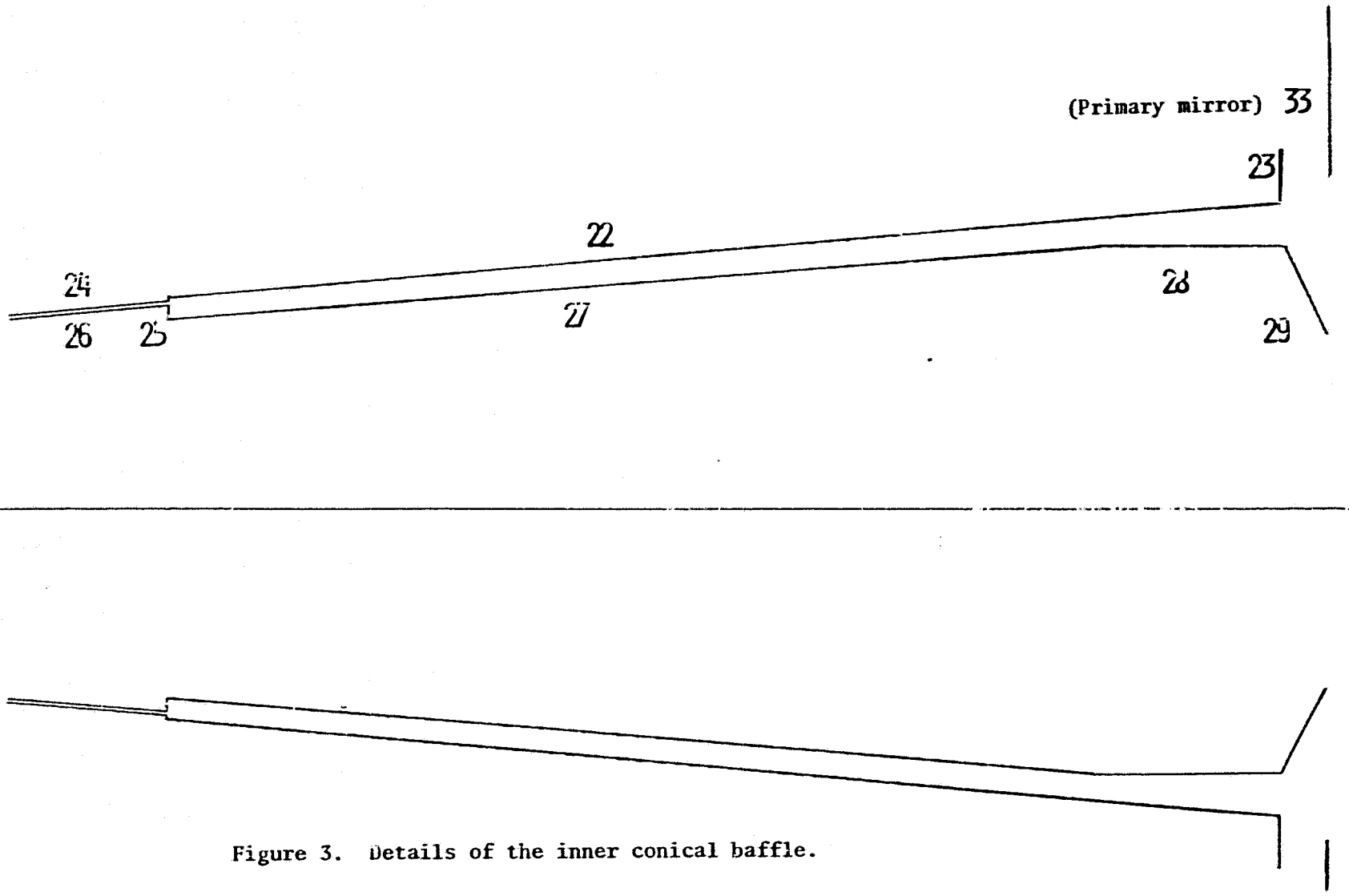

Figure 3. Details of the inner conical baffle.

TABLE 2. CRITICAL OBJECTS

21.01	BACK OF STRUT
42.01	SECONDARY BAFFLE
43.01	SECONDARY BAFFLE
14.01	RIGHT SIDE OF APERTURE STOP
33.02	PRIMARY MIRROR
32.03	SECONDARY MIRROR
36.02	DAMAGED AREA OF PRIMARY MIRROR
26.02	END OF INNER CONICAL
27.02	MIDDLE OF INNER CONICAL
28.02	RIGHT SIDE OF INNER CONICAL
29.02	RIGHT END OF INNER CONICAL
19.02	SECONDARY BAFFLE
7.02	"
15.02	"
17.02	"
34.02	"
37.02	"
39.02	"
41.02	"
43.02	"
46.03	STIMULATOR
20.03	SECONDARY BAFFLE IN SPACE 3
19.03	"

.01 OBJECT IN SPACE ONE (OBJECT TO PRIMARY)
.02 OBJECT IN SPACE TWO (PRIMARY TO SECONDARY)
.03 OBJECT IN SPACE THREE (SECONDARY TO IMAGE)

ADDITIONAL OBJECTS FOR VISIBLE DETECTORS

26.03	RIGHT SIDE OF INNER CONICAL
27.03	MIDDLE OF INNER CONICAL
28.03	RIGHT SIDE OF INNER CONICAL

is located just behind the secondary mirror. The main benefit of this design is that the detectors do not see the primary cone baffle nor part of the secondary baffle directly. Although both of these objects are seen in reflection through the secondary mirror, the high forward-scatter path from the primary cone baffle is eliminated. The visible detectors do not have field masks and field lenses; hence these power transfer mechanisms do exist for these detectors, and their OAR will be worse than for the IR detectors.

Sunshade

The orientation of the sunshade relative to the struts holding the secondary and the two point-source angle scans is shown in Figure 4. The top view depicts the scan called 180° throughout the report while the bottom view shows the 90° azimuth scan. The location of the damaged area on the primary mirror is also indicated. The sunshade cone was sliced off at 31° in the orientation shown and an elliptical tilted aperture was used to properly obscure the beam. The earth is considered to be in the +y direction with the sun being nominally in the -y direction. It should be mentioned also that we are doing no analysis for points in the -y scan direction. The results of this set of angles (if ever done) would, of course be, dramatically different than for the +y scan because the sunshade will change the illumination for angles greater than about 40°. Other implications of not doing this set of angles will be discussed in the section on Earth integration.

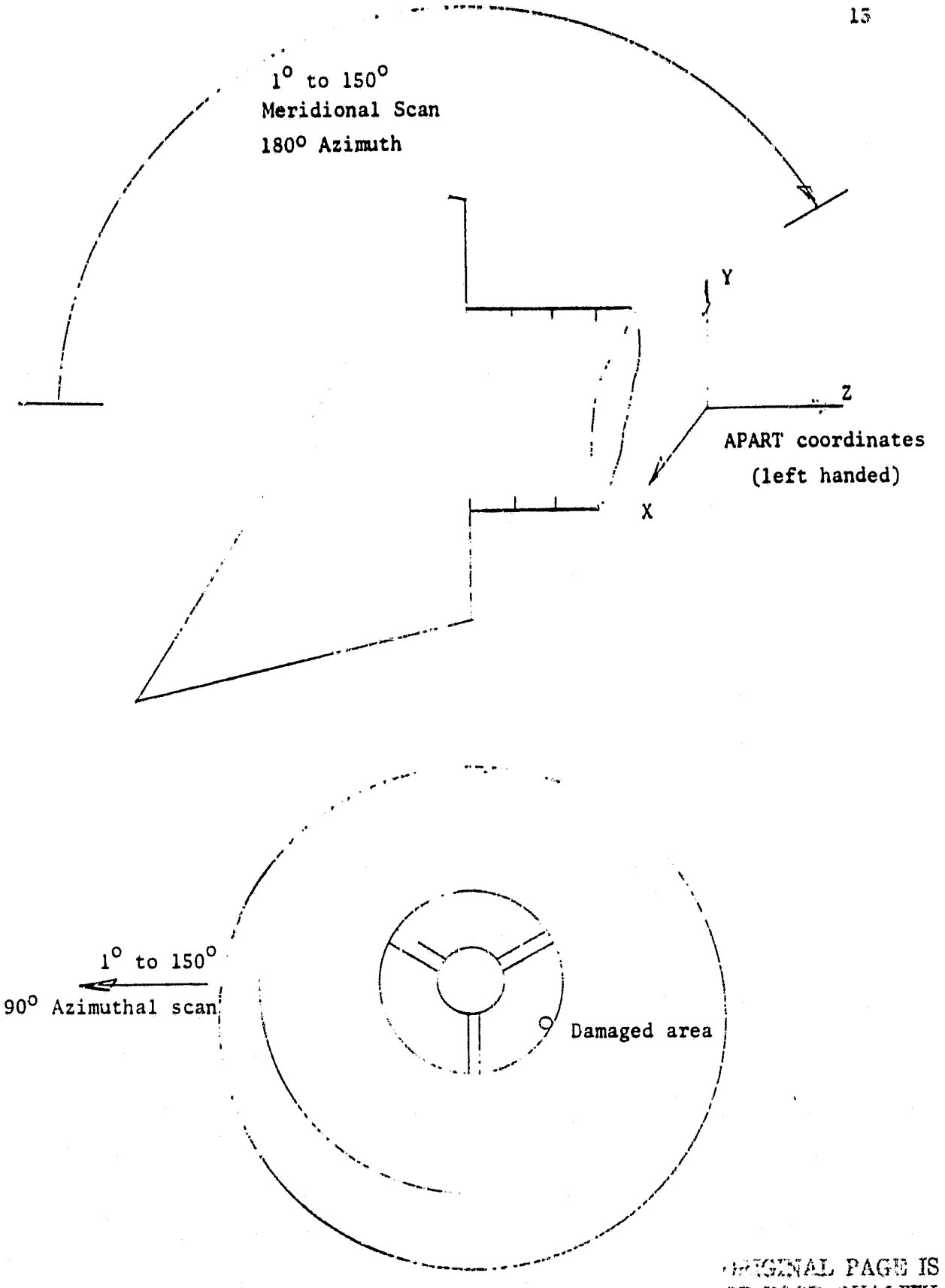

Figure 4. Sensor orientation and scan directions.

Another effect of the sunshade is that it will reflect radiation into the telescope entrance port at some angles. A complete description on this phenomenon is to be found in the 1978 report including the results of measurements on a sunshade model. Although more radiation enters the entrance port from angles of 0^{o} to 50^{o}, the increased energy is measurable at the detector only for a small range of angles from 40^{o} to 45^{o}.

At angles up to 40^{o} direct radiation strikes either a critical object (e.g. the primary mirror for angles up to 20^{o}) or object 8. Object 8 has no vanes on it; thus it scatters a larger proportion of energy to the critical objects than light incident on objects 5 and 6, which have vanes on them. Therefore, even though objects 5 and 6 are illuminated for angles up to 40^{o} by direct and reflected radiation, they contribute an insignificant amount of the total energy falling on the detector because the other paths are higher attenuation paths.

At 40^{o} and 45^{o} only objects 5 and 6 are illuminated by direct and reflected light so now the energy falling on the detector is increased proportionally to how much additional radiation is reflected onto them. Based upon the measured data, the increase amounts to 1.40 at 40^{o} and 1.18 at 45^{o}. The plotted $A(\theta)$ will reflect this increase at the two angles.

Diffraction Transfers

NASA/ARC directed BRO to calculate the irradiance on the focal plane from diffraction off the front aperture and subsequent scatter.

The front aperture edge is called object 47 in the analysis. At angles up to 80°, in the 180° azimuth, this edge can be directly illuminated and energy will diffract around it to the critical objects listed in Table 2. At the 90° azimuth the direct illumination is blocked off at angles greater than 60°. At larger off axis angles multiple diffraction transfers were considered (see Figure 5). From 88° to 120° double diffraction was considered with the first diffraction occurring at object 50 and the second at object 47. Object 2 (the sunshade) could also be directly illuminated over these angles and could scatter radiation back to object 5 and 6 and subsequently to the critical objects. At still larger angles of 130° to 150°; triple diffraction was calculated with the first diffraction occuring at the outer sunshade tip(object 30). The second diffraction is at object 50 which will bend the light around to the sunshade (object 2) and the front aperture edge (object 47). The path from object 50 to object 2 and subsequent scatter was not considered because that path would require one more level of scatter for radiation to reach the image compared to the path from object 50 to object 47.

3.0 BRDF MODELS

Mirror Scattering

The mirror scattering model used in APART is described in the 1979 report and is based upon observations of measured data. In Appendix A there is a discussion of the measured data for the primary and its damaged area as well as the fit data for the APART model. The

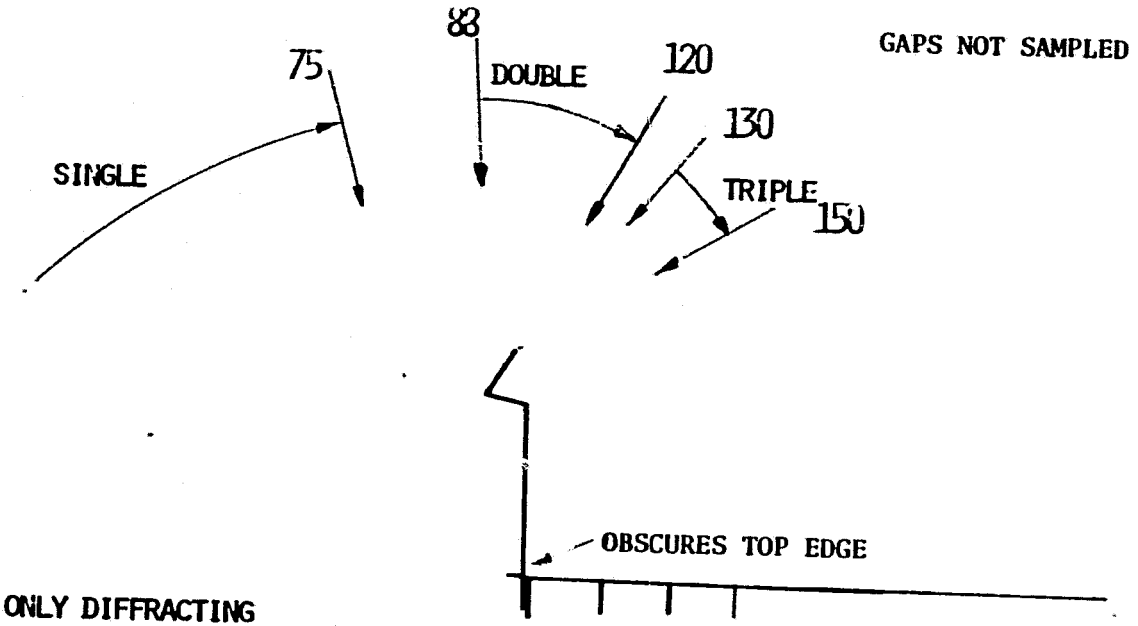

Figure 5. Diffraction levels and angles.

secondary mirror has not been measured at this time, so the model used was the same as that used in the previous analysis. A summary of the scattering properties of the mirrors are listed in Table 3.

Table 3. Scattering Model of Mirrors

Element	BRDF at $\beta - \beta_o = .01$	Slope	Wavelength	Fit Factor
secondary	1.75 E-3	-1.	10.6	
secondary	4.14 E-1	-1.	vis.	
primary	7.33 E-3	- .727	10.6	0.968
primary	6.98	-2.674	vis.	0.97f
damaged area	4.07	-1.682	10.6	0.980

For comparison, the model used for the primary mirror in the previous analysis is the same as for the secondary now. Thus, the primary is measured to be about four times worse than expected at small angles (1^o) and nine times worse at an angle of 10^o.

An analysis of the damaged area, done in September 1979, used a BRDF of 1.75 at $\beta - \beta_o = .01$ and a slope of either -1.0 or -2.0. The model used in this analysis was based upon measurements of the damaged area, with the present BRDF being slightly higher and a slope within the range speculated before.

The BRDF models used are plotted on the original BRDF plots for the primary at 0.6328 μ and 10.6 μ and the damaged area at 10.6 μ in Figures 6, 7, and 8.

Black surfaces

The black surfaces were assumed to be coated with Martin Black having the scattering properties as described in the 1978 report and briefly

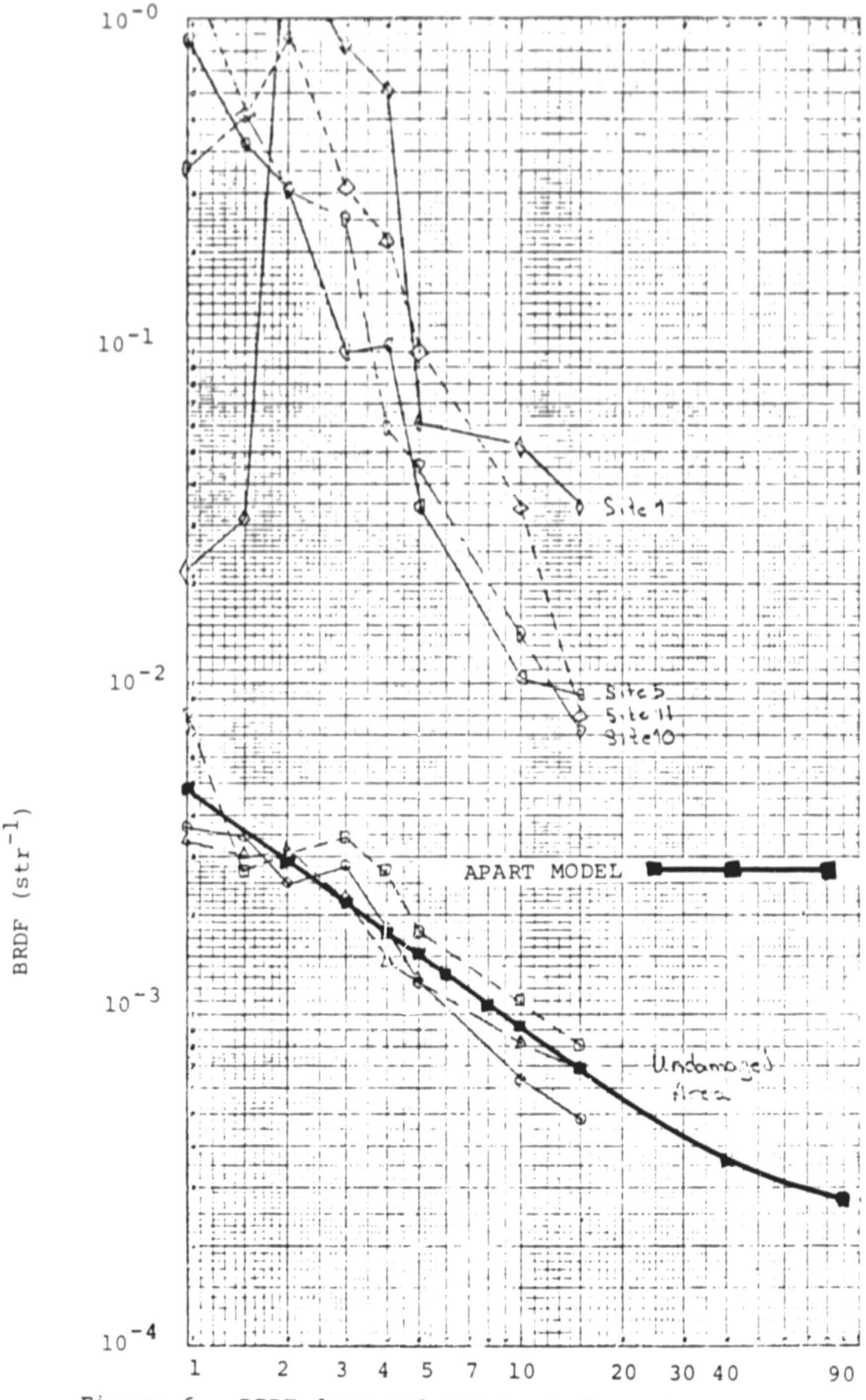

Figure 6. BRDF data and model of the primary mirror at 10.6μm.

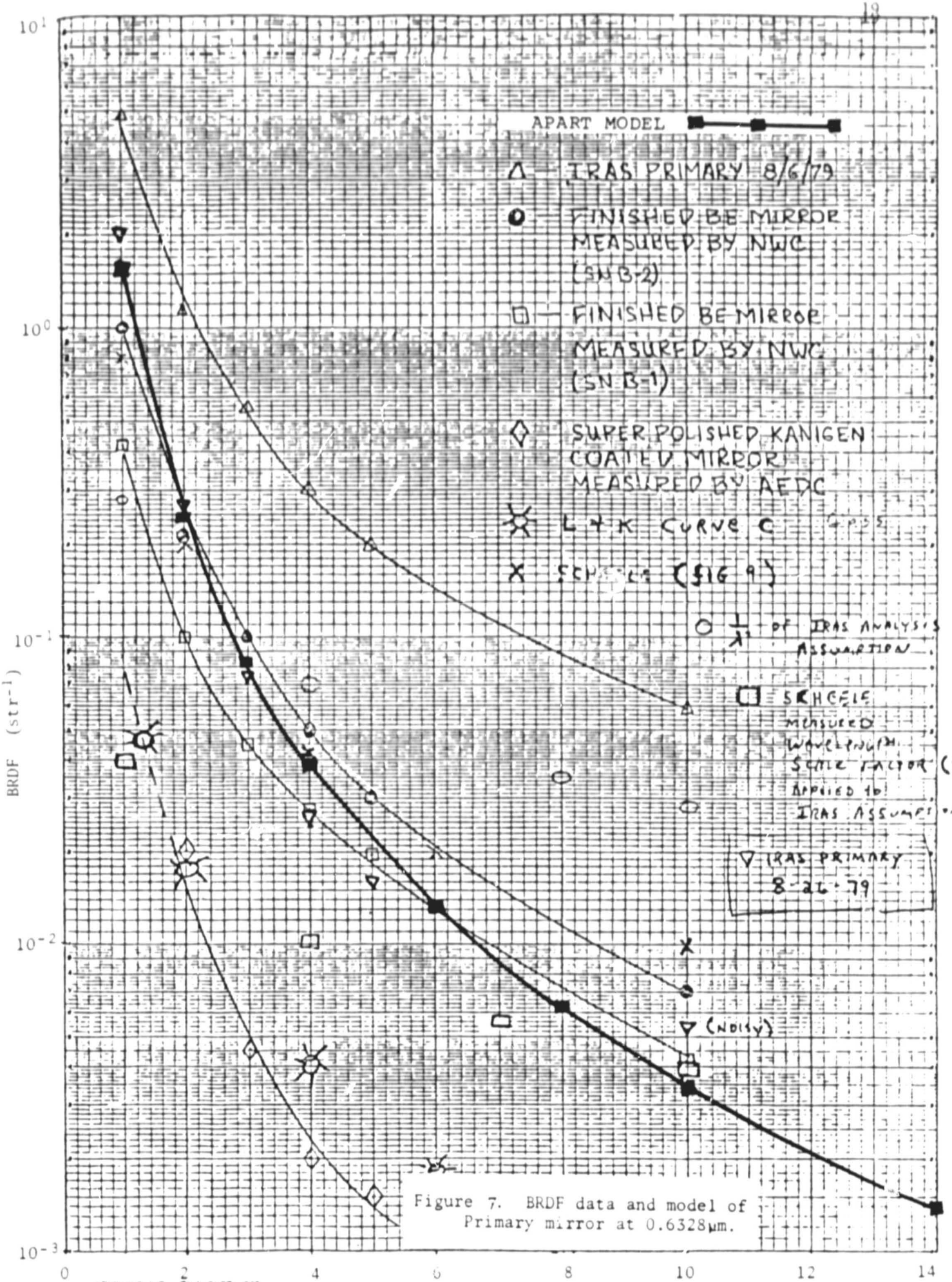

Figure 7. BRDF data and model of Primary mirror at 0.6328μm.

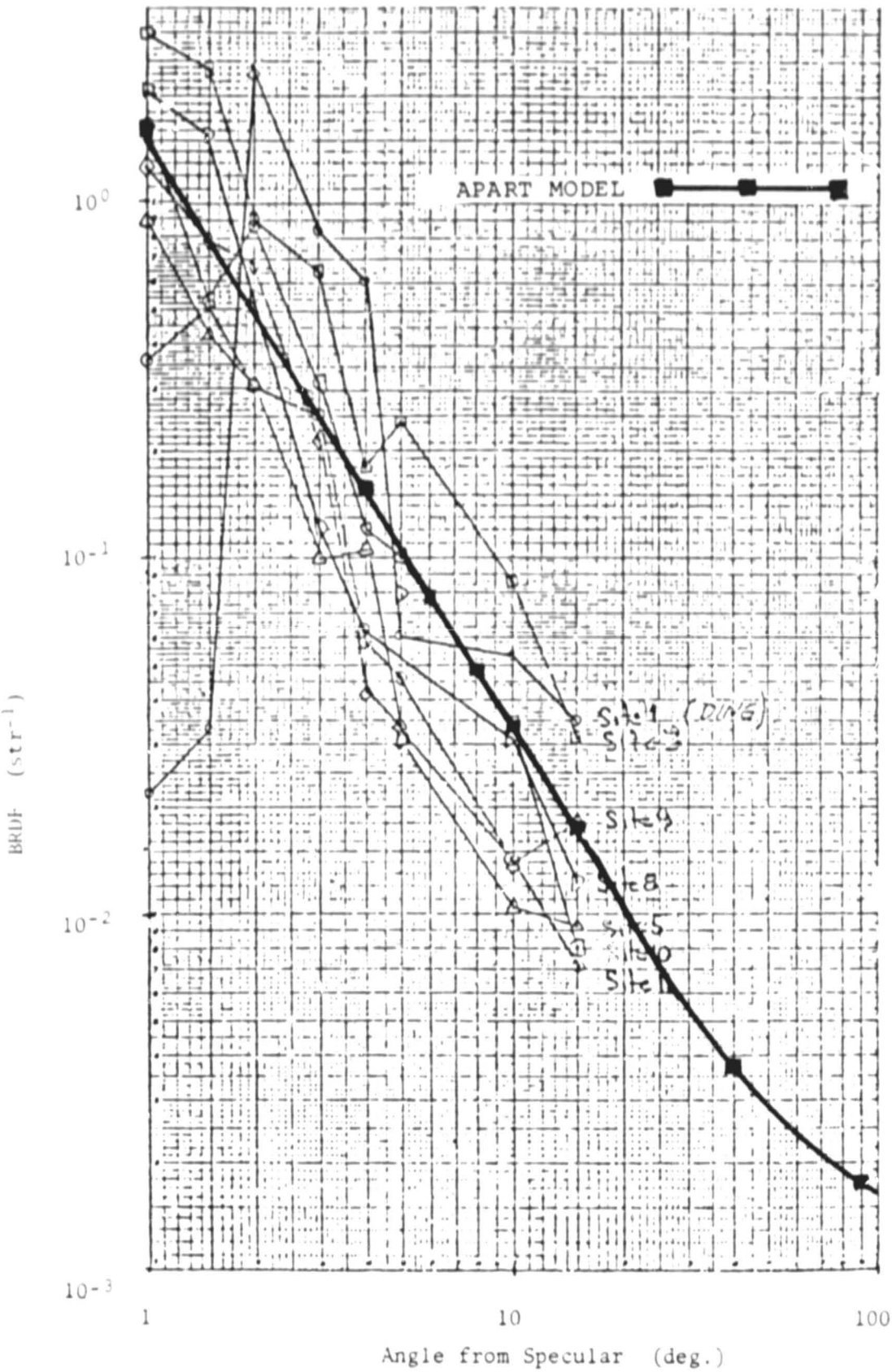

Figure 8. BRDF data and model of damaged area at 10.6μm.

repeated in Appendix A.

Sunshade surface

For scattering purposes, the sunshade was assumed to be a 0.05 Lambertian surface. The previous analysis used a 0.001 reflectance, which was probably too low because of the contaminants that are bound to be on the Gold coating.

4.0 BRDF SCALING

Mirrors

The mirror scaling algorithm reported by Harvey[1] accounts for the grating effect and the resultant magnitude is:

$$s(a\beta) = \frac{1}{a^{4+m}}\ s(\beta)$$

where "a" is the wavelength change during the scaling and "m" is the slope of the BRDF in $\beta - \beta_o$ space. This scaling rule is valid over short wavelength changes and where the scattering mechanism is from the RMS roughness on the surface. At longer IR wavelengths the scattering mechanism changes to surface particulate scattering, in which case the rule is probably no longer valid. However, there are no BRDF measurements on mirrors beyond 10.6μ on which to empirically base another scaling rule, so we have elected to use the Harvey rule. See Table 4 for the ratio of mirror scattering to the 10.6μ measured data for the two mirrors and the damaged area.

Table 4. Wavelength scaling for mirrors.

	Ratio to 10.6 data		
Mirror	22.5	64.5	102.5 Microns
Primary	8.55 E-2	2.72 E-3	5.95 E-4
Damaged Area	1.75 E-1	1.52 E-2	5.20 E-3
Secondary	1.05 E-1	4.45 E-3	1.11 E-3

Blacks

We have elected not to do any wavelength scaling for the black surfaces in IRAS because there is no available indication of how the scaling should be done. Measurements of total hemispherical diffuse scattering off of Martin Black have been made, but the results are inconsistent. Furthermore, if the total hemispherical scattering does change, then there still is no indication of how the BRDF reflects the change. In the previous analysis we did scale up the Martin Black by a factor of 10. In any case, the validity of the longer wavelengths analysis is questionable. The 1978 report contains more information concerning this problem.

Sunshade

The scattering remained the same for all wavelengths for the sunshade.

5.0 THERMAL EMISSION

The contribution of energy in the focal plane from thermal emission off the sunshade and subsequent scatter was calculated using APART. The temperature of the sunshade was assumed to be $80^{o}K$ with an

emissivity of 0.02. First, the radiant exitance was calculated in each waveband for the $80^{\circ}K$ as well as $10^{\circ}K$ and $4^{\circ}K$ for comparison (see Table 5).

Table 5. Radiant exitance for thermal emission.

T	8-15μ	15-30μ	48-81μ	87-118μ
$80^{\circ}K$	5.11×10^{-7}	3.25×10^{-5}	7.59×10^{-5}	2.23×10^{-5} (w/cm^2)
ratio to total	0.0022	0.140	0.327	0.097
$4^{\circ}K$				4.53×10^{-19} (w/cm^2)
$10^{\circ}K$				1.05×10^{-10} (w/cm^2)

Note: emissivity = 1.0 for all cases.

It should be noted that if any interior parts of the telescope reach a temperature of about $10^{\circ}K$ they will probably contribute more power to the image than the sunshade does. This is because the sunshade's emitted radiation is highly attenuated before it reaches the focal plane, whereas most interior surfaces have at least 10^4 less attenuation. These probabilities, combined with the ratio of emissivities (99% blacks to 2% sunshade), more than make up the 10^{-5} radiance difference. If the expected low temperatures for the rest of the system can be achieved, the sunshade will be the major contributor of thermally emitted radiation.

To complete the thermal radiation analysis the emissivity was multiplied by the radiance and the sunshade area to arrive at the total power radiated. This power was transferred through the system in an identical manner as scattered radiation is calculated.

6.0 ANALYSIS RESULTS

The results of the scatter and diffraction analysis are presented in two complementary forms: First, a percent table is given for each set of ten angles, wavelength, and azimuth. There are 19 of these percent tables covering these cases (Tables 6 through 24). Second, the A(θ) is plotted for a number of select combinations (Figures 9 through 17).

Percent Tables

The left column contains the object number as shown in Figures 1, 2, and 3 with a literal description following it. The columns that follow contain the percent of contribution of each object to the total power reaching the image for each angle. The contribution is only for the final level of scatter, and thus only the critical objects appear in the percent tables. The tables are shown for the addition of scatter and diffraction. The table for visible wavelength and the first ten angles is identical for both azimuths because the damaged area's contribution was integrated into the BRDF of the primary mirror.

A(θ) Plot

The total power row in the percent table represents the power reaching an individual detector located on-axis for an incident radiation of 1 W/cm^2 measured normal to the incident wavefront. To get A(θ), this number must be divided by the solid angle of the detector (2.856×10^{-7}) and the power in (2394.4 watts), yielding a factor of 1462 to multiply by. All of the A(θ) plots are for the sum of scatter and diffraction.

7 SEC. DISK 3	0.00	0.00	0.00	0.00	0.00	0.00	.02	.22	.12	.03
12 LEFT APT.	0.00	0.00	.00	.05	1.35	10.65	57.27	0.00	0.00	0.00
14 RIGHT APT.	0.00	0.00	0.00	0.00	0.00	1.02	39.55	0.00	0.00	0.00
15 SEC. CONE 4	0.00	0.00	0.00	0.00	0.00	0.00	.04	.23	.11	.04
17 SEC. CONE 5	0.00	0.00	0.00	.01	0.00	0.00	.04	.31	.14	.05
19 SEC. CONE 1	0.00	0.00	0.00	77.58	0.00	0.00	.14	1.04	.58	.21
20 SEC. APT	0.00	0.00	2.01	2.39	0.00	0.00	.04	.27	.12	0.00
21 STRUT BACK	.00	.00	.00	0.00	.09	.49	0.00	.03	.03	.02
25 INNER TIP END	.01	0.00	0.00	0.00	0.00	0.00	0.00	0.00	0.00	0.00
26 LEFT INNER CONICAL	0.00	0.00	0.00	0.00	0.00	0.00	.25	1.97	2.19	3.02
27 MIDDLE INNER CON.	0.00	0.00	0.00	0.00	0.00	0.00	.92	7.30	8.21	11.35
28 RIGHT INNER CON.	.00	0.00	0.00	0.00	0.00	0.00	0.00	0.00	0.00	0.00
29 RIGHT INNER C END	.04	0.00	0.00	0.00	0.00	0.00	0.00	0.00	0.00	0.00
32 SECONDARY MIRROR	42.94	62.92	71.62	12.55	0.00	0.00	.31	1.93	.65	.17
33 PRIMARY MIRROR	56.59	36.48	25.69	6.57	50.45	66.33	.37	25.08	29.44	24.46
34 SEC. CONE 6	0.00	0.00	0.00	.01	0.00	.01	.07	.50	.31	.12
36 DAMAGED AREA	.41	.56	.62	.30	7.32	21.49	.76	20.44	19.97	19.24
37 SEC. CONE 7	0.00	0.00	0.00	.01	0.00	.01	.07	15.72	15.56	14.49
39 SEC. CONE 8	0.00	0.00	0.00	0.00	0.00	0.00	.02	.17	.08	.03
41 SEC. CONE 9	0.00	0.00	0.00	.01	2.17	.01	.07	.81	.51	.39
42 SEC. DISK 9	0.00	0.00	0.00	.04	1.28	0.00	0.00	.27	.26	.28
43 SEC. CONE 10	0.00	0.00	0.00	0.00	37.34	0.00	.04	21.63	21.69	24.56
46 STIMULATOR	.01	.05	.06	0.00	0.00	0.00	0.00	0.00	0.00	0.00
TOTAL POWER	.231E-02	.496E-03	.221E-03	.192E-03	.239E-05	.304E-06	.318E-07	.520E-08	.548E-08	.423E-08
SOURCE ANG	1.0	2.0	3.0	5.0	10.0	15.0	20.0	25.0	30.0	35.0

Table 6. Percent Table, 1st 10 angles, 180° azimuth, visible.

7 SEC. DISK 3	0.00	0.00	0.00	0.00	0.00	0.00	.01	.23	.11	.04
12 LEFT APT.	0.00	0.00	.06	.06	2.17	14.95	30.71	0.00	0.00	0.00
14 RIGHT APT.	0.00	0.00	0.00	0.00	0.00	1.42	21.21	0.00	0.00	0.00
15 SEC. CONE 4	0.00	0.00	0.00	0.00	0.00	0.00	.02	.24	.12	.05
17 SEC. CONE 5	0.00	0.00	0.00	.01	0.00	0.00	.02	.36	.16	.06
19 SEC. CONE 1	0.00	0.00	0.00	97.24	.07	.06	.13	1.45	.75	.45
20 SEC. APT	0.00	0.00	55.72	1.64	0.00	0.00	.01	.13	.07	0.00
21 STRUT BACK	.01	.03	.03	0.00	.15	.68	0.00	.04	.03	.03
25 INNER TIP END	.83	0.00	0.00	0.00	0.00	0.00	0.00	0.00	0.00	0.00
28 RIGHT INNER CON.	.04	0.00	0.00	0.00	0.00	0.00	0.00	0.00	0.00	0.00
29 RIGHT INNER C END	4.48	0.00	0.00	0.00	0.00	0.00	0.00	0.00	0.00	0.00
32 SECONDARY MIRROR	22.74	21.00	8.40	.07	.00	.00	.00	.01	.00	.00
33 PRIMARY MIRROR	19.36	31.09	17.00	.53	20.35	52.95	47.30	23.19	33.89	24.91
34 SEC. CONE 6	0.00	0.00	0.00	.01	0.00	.01	.04	.59	.34	.13
36 DAMAGED AREA	51.30	44.09	17.18	.37	11.75	30.01	.44	23.46	22.19	22.43
37 SEC. CONE 7	0.00	0.00	0.00	.01	0.00	.01	.04	19.11	17.95	19.71
39 SEC. CONE 8	0.00	0.00	0.00	0.00	0.00	0.00	.01	.19	.09	.03
41 SEC. CONE 9	0.00	0.00	0.00	.01	3.48	.01	.04	.93	.57	.45
42 SEC. DISK 9	0.00	0.00	0.00	.05	2.06	.00	.00	.31	.29	.34
43 SEC. CONE 10	0.00	0.00	0.00	0.00	59.97	.00	.02	24.74	24.05	27.35
46 STIMULATOR	1.24	3.79	1.61	0.00	0.00	0.00	0.00	0.00	.00	.00
TOTAL POWER	.184E-04	.628E-05	.797E-05	.153E-03	.148E-05	.218E-06	.593E-07	.455E-08	.494E-08	.354E-08
SOURCE ANG	1.0	2.0	3.0	5.0	10.0	15.0	20.0	25.0	30.0	35.0

Table 7. Percent Table, 1st 10 angles, 180° azimuth, 11.5μm.

7 SEC. DISK 3	0.00	0.00	0.00	0.00	0.00	0.00	.02	.41	.22	.07
12 LEFT APT.	0.00	0.00	.10	.06	3.02	55.26	54.42	.00	.00	.00
14 RIGHT APT.	0.00	0.00	0.00	0.00	0.00	5.28	37.58	0.00	.00	.00
15 SEC. CONE 4	0.00	0.00	0.00	0.00	0.00	0.00	.04	.47	.24	.09
17 SEC. CONE 5	0.00	0.00	0.00	.01	0.00	0.00	.04	.65	.31	.11
19 SEC. CONE 1	0.00	0.00	0.00	98.08	.19	.41	.32	3.20	1.78	1.02
20 SEC. APT	0.00	0.00	89.76	1.65	0.00	0.00	.02	.23	.14	0.00
21 STRUT BACK	.05	.18	.05	0.00	.21	2.53	0.00	.07	.06	.04
25 INNER TIP END	4.23	0.00	0.00	0.00	0.00	0.00	0.00	0.00	0.00	0.00
28 RIGHT INNER CON.	.20	0.00	0.00	0.00	0.00	0.00	0.00	0.00	0.00	0.00
29 RIGHT INNER C END	22.83	0.00	0.00	0.00	0.00	0.00	0.00	0.00	0.00	0.00
32 SECONDARY MIRROR	12.17	13.45	1.41	.01	.00	.00	.00	.00	.00	.00
33 PRIMARY MIRROR	8.44	16.21	2.32	.05	2.43	16.84	7.17	4.35	5.72	4.04
34 SEC. CONE 6	0.00	0.00	0.00	.01	0.00	.04	.07	1.24	.67	.25
36 DAMAGED AREA	45.76	47.05	4.79	.07	2.87	19.56	.14	7.45	7.66	6.89
37 SEC. CONE 7	0.00	0.00	0.00	.01	0.00	.04	.07	34.57	33.97	34.57
39 SEC. CONE 8	0.00	0.00	0.00	0.00	0.00	0.00	.02	.34	.18	.05
41 SEC. CONE 9	0.00	0.00	0.00	.01	4.85	.04	.07	1.67	1.12	.79
42 SEC. DISK 9	0.00	0.00	0.00	.05	2.87	.00	.00	.56	.57	.60
43 SEC. CONE 10	0.00	0.00	0.00	0.00	83.57	.01	.04	44.76	47.37	51.49
46 STIMULATOR	6.32	23.11	2.57	0.00	0.00	0.00	0.00	0.00	.00	.00
TOTAL POWER	.361E-05	.103E-05	.500E-05	.152E-03	.106E-05	.586E-07	.335E-07	.252E-08	.251E-08	.202E-08
SOURCE ANG	1.0	2.0	3.0	5.0	10.0	15.0	20.0	25.0	30.0	35.0

Table 8. Percent Table, 1st 10 angles, 180° azimuth, 22.5μm.

7 SEC. DISK 3	0.00	0.00	0.00	0.00	0.00	0.00	.02	.45	.24	.08
12 LEFT APT.	0.00	0.00	.10	.06	3.17	83.02	58.31	.01	.01	.01
14 RIGHT APT.	0.00	0.00	0.00	0.00	0.00	7.93	40.27	0.00	.00	.00
15 SEC. CONE 4	0.00	0.00	0.00	0.00	0.00	0.00	.04	.51	.27	.10
17 SEC. CONE 5	0.00	0.00	0.00	.01	0.00	0.00	.04	.71	.35	.12
19 SEC. CONE 1	0.00	0.00	0.00	98.19	.56	1.67	.75	5.89	3.31	2.08
20 SEC. APT	0.00	0.00	96.46	1.66	0.00	0.00	.02	.26	.16	0.00
21 STRUT BACK	.13	.64	.05	0.00	.22	3.80	0.00	.08	.07	.04
25 INNER TIP END	11.02	0.00	0.00	0.00	0.00	0.00	0.00	0.00	0.00	0.00
28 RIGHT INNER CON.	.53	0.00	0.00	0.00	0.00	0.00	0.00	0.00	0.00	0.00
29 RIGHT INNER C END	59.47	0.00	0.00	0.00	0.00	0.00	0.00	0.00	0.00	0.00
32 SECONDARY MIRROR	1.34	2.00	.06	.00	.00	.00	.00	.00	.00	.00
33 PRIMARY MIRROR	.70	1.81	.08	.00	.08	.81	.24	.15	.21	.14
34 SEC. CONE 6	0.00	0.00	0.00	.01	0.00	.06	.08	1.36	.75	.27
36 DAMAGED AREA	10.35	14.36	.45	.01	.26	2.56	.01	.72	.75	.66
37 SEC. CONE 7	0.00	0.00	0.00	.01	0.00	.06	.08	37.89	38.31	38.12
39 SEC. CONE 8	0.00	0.00	0.00	0.00	0.00	0.00	.02	.37	.20	.06
41 SEC. CONE 9	0.00	0.00	0.00	.01	5.08	.06	.08	1.94	1.26	.87
42 SEC. DISK 9	0.00	0.00	0.00	.05	3.01	.00	.00	.62	.65	.66
43 SEC. CONE 10	0.00	0.00	0.00	0.00	87.62	.04	.05	49.12	53.45	56.80
46 STIMULATOR	16.46	81.19	2.79	0.00	0.00	0.00	0.00	0.00	.00	.00
TOTAL POWER	.139E-05	.293E-06	.460E-05	.152E-03	.101E-05	.390E-07	.313E-07	.230E-08	.223E-08	.183E-08
SOURCE ANG	1.0	2.0	3.0	5.0	10.0	15.0	20.0	25.0	30.0	35.0

Table 9. Percent Table, 1st 10 angles, 180° azimuth, 65.5μm.

7 SEC. DISK 3	0.00	0.00	0.00	0.00	0.00	0.00	.02	.45	.24	.08
12 LEFT APT.	0.00	0.00	.10	.06	3.16	84.15	58.21	.02	.01	.01
14 RIGHT APT.	0.00	0.00	0.00	0.00	0.00	8.04	40.20	0.00	.00	.00
15 SEC. CONE 4	0.00	0.00	0.00	0.00	0.00	0.00	.04	.50	.26	.10
17 SEC. CONE 5	0.00	0.00	0.00	.01	0.00	0.00	.04	.70	.35	.12
19 SEC. CONE 1	0.00	0.00	0.00	98.19	.90	2.66	1.10	7.92	4.47	2.93
20 SEC. APT	0.00	0.00	96.86	1.66	0.00	0.00	.02	.25	.15	0.00
21 STRUT BACK	.14	.73	.05	0.00	.22	3.55	0.00	.08	.07	.04
25 INNER TIP END	12.02	0.00	0.00	0.00	0.00	0.00	0.00	0.00	0.00	0.00
28 RIGHT INNER CON.	.58	0.00	0.00	0.00	0.00	0.00	0.00	0.00	0.00	0.00
29 RIGHT INNER C END	64.90	0.00	0.00	0.00	0.00	0.00	0.00	0.00	0.00	0.00
32 SECONDARY MIRROR	.36	.57	.02	.00	.00	.00	.00	.00	.00	.00
33 PRIMARY MIRROR	.17	.45	.02	.00	.02	.18	.05	.03	.04	.03
34 SEC. CONE 6	0.00	0.00	0.00	.01	0.00	.06	.08	1.34	.75	.27
36 DAMAGED AREA	3.86	5.60	.16	.00	.09	.89	.01	.24	.26	.23
37 SEC. CONE 7	0.00	0.00	0.00	.01	0.00	.06	.03	37.28	38.09	37.95
39 SEC. CONE 8	0.00	0.00	0.00	0.00	0.00	0.00	.02	.37	.20	.06
41 SEC. CONE 9	0.00	0.00	0.00	.01	5.08	.06	.08	1.81	1.25	.87
42 SEC. DISK 9	0.00	0.00	0.00	.05	3.00	.00	.00	.62	.65	.66
43 SEC. CONE 10	0.00	0.00	0.00	0.00	87.53	.06	.06	48.39	53.18	56.63
46 STIMULATOR	17.96	92.64	2.80	0.00	0.00	0.00	0.00	0.00	.00	.00
TOTAL POWER	.127E-05	.257E-06	.459E-05	.152E-03	.101E-05	.385E-07	.313E-07	.233E-08	.224E-08	.184E-08
SOURCE ANG	1.0	2.0	3.0	5.0	10.0	15.0	20.0	25.0	30.0	35.0

Table 10. Percent Table, 1st 10 angles, 180° azimuth, 102.5μm.

7 SEC. DISK 3	.00	0.00	0.00	0.00	0.00	.00	.00	.00
12 LEFT APT.	.01	.01	.23	.18	.12	.03	.02	.02
14 RIGHT APT.	.01	.01	.09	.07	.04	.01	.01	.01
15 SEC. CONE 4	.00	0.00	0.00	0.00	0.00	.00	.00	.00
17 SEC. CONE 5	.00	.00	.02	.02	0.00	.00	.00	.00
19 SEC. CONE 1	.90	.90	30.83	29.77	26.96	4.00	1.40	1.30
20 SEC. APT	.01	.01	1.29	1.19	.98	.20	.10	.10
21 STRUT BACK	.00	.00	.02	.02	.02	.00	.00	.00
25 INNER TIP END	.00	.00	0.00	0.00	0.00	.00	.00	.00
26 LEFT INNER CONICAL	20.29	19.41	5.75	5.86	6.00	17.98	19.67	19.99
27 MIDDLE INNER CON.	77.56	78.34	12.99	13.60	14.86	71.12	76.78	76.76
32 SECONDARY MIRROR	.70	.80	28.45	28.38	27.94	3.80	1.20	1.10
33 PRIMARY MIRROR	.50	.50	19.83	20.44	22.63	2.80	.80	.70
34 SEC. CONE 6	.00	.00	0.00	0.00	0.00	.00	.00	.00
37 SEC. CONE 7	.00	.00	0.00	0.00	0.00	.00	.00	.00
41 SEC. CONE 9	.00	.00	.02	0.00	0.00	.00	.00	.00
42 SEC. DISK 9	.00	.00	.05	.04	.04	.01	.00	.00
43 SEC. CONE 10	.01	.01	.43	.42	.40	.06	.02	.02
46 STIMULATOR	0.00	0.00	0.00	0.00	0.00	.00	0.00	0.00
TOTAL POWER	.982E-09	.804E-09	.165E-10	.158E-10	.148E-10	.165E-11	.795E-12	.958E-13
SOURCE ANG	40.0	45.0	55.0	60.0	75.0	88.0	110.0	120.0

Table 11. Percent Table, 2nd 10 angles, 180° azimuth, visible.

7 SEC. DISK 3	.11	0.00	0.00	0.00	0.00	.10	.20	.30	0.00	0.00
12 LEFT APT.	1.22	1.26	.90	.74	.58	1.38	1.90	2.00	.30	.40
14 RIGHT APT.	.49	.56	.34	.25	.18	.49	.80	.90	0.00	0.00
15 SEC. CONE 4	.11	0.00	0.00	0.00	0.00	.10	.20	.30	0.00	0.00
17 SEC. CONE 5	.06	.08	.09	.09	0.00	.10	.10	.10	0.00	0.00
19 SEC. CONE 1	73.27	69.24	72.06	73.30	74.54	80.15	78.90	78.08	57.72	58.27
20 SEC. APT	.94	1.36	1.19	.96	.74	2.46	2.20	2.20	.10	.60
21 STRUT BACK	.11	.08	.09	.09	.09	.10	.20	.20	0.00	0.00
25 INNER TIP END	.17	.16	0.00	0.00	0.00	.10	.30	.30	0.00	0.00
26 LEFT INNER CONICAL	.06	0.00	0.00	0.00	0.00	0.00	.10	.10	0.00	0.00
32 SECONDARY MIRROR	.49	.54	.53	.53	.61	.80	.60	.60	.70	.70
33 PRIMARY MIRROR	7.33	7.49	6.34	5.79	5.04	9.41	10.80	11.19	4.31	5.02
34 SEC. CONE 6	.06	.08	0.00	0.00	0.00	.10	.10	.10	0.00	0.00
36 DAMAGED AREA	13.37	16.99	16.29	16.15	16.03	1.24	.71	.83	34.87	32.60
37 SEC. CONE 7	.06	.08	0.00	0.00	0.00	.10	.10	.10	0.00	0.00
41 SEC. CONE 9	.06	.08	.09	0.00	0.00	.10	.10	.10	0.00	0.00
42 SEC. DISK 9	.20	.18	.19	.19	.19	.30	.30	.30	.10	.20
43 SEC. CONE 10	1.88	1.78	1.99	1.89	1.99	2.88	2.40	2.30	1.80	2.11
46 STIMULATOR	.04	.02	.02	.01	.01	.10	.00	.00	.10	.10
TOTAL POWER	.129E-10	.717E-11	.443E-11	.402E-11	.321E-11	.330E-13	.640E-14	.755E-15	.185E-23	.183E-24
SOURCE ANG	40.0	45.0	55.0	60.0	75.0	88.0	110.0	120.0	130.0	150.0

Table 12. Percent Table, 2nd 10 angles, 180° azimuth, 11.5μm.

7 SEC. DISK 3	.09	0.00	0.00	0.00	0.00	.11	.22	.34	0.00	0.00
12 LEFT APT.	1.23	1.45	1.05	.87	.69	1.51	2.13	2.25	.45	.59
14 RIGHT APT.	.45	.62	.38	.30	.21	.53	.90	1.01	0.00	0.00
15 SEC. CONE 4	.09	0.00	0.00	0.00	0.00	.11	.22	.34	0.00	0.00
17 SEC. CONE 5	.05	.09	.09	.10	0.00	.11	.11	.11	0.00	0.00
19 SEC. CONE 1	90.32	87.69	89.39	90.23	91.07	89.30	88.64	88.18	86.58	85.83
20 SEC. APT	.80	1.50	1.33	1.08	.85	2.66	2.47	2.48	.15	.89
21 STRUT BACK	.09	.09	.09	.10	.11	.11	.22	.23	0.00	0.00
25 INNER TIP END	.14	.18	0.00	0.00	0.00	.11	.34	.34	0.00	0.00
26 LEFT INNER CONICAL	.05	0.00	0.00	0.00	0.00	0.00	.11	.11	0.00	0.00
32 SECONDARY MIRROR	.07	.08	.07	.07	.08	.09	.07	.07	.11	.11
33 PRIMARY MIRROR	.69	.78	.66	.61	.53	.89	1.04	1.08	.55	.63
34 SEC. CONE 6	.05	.09	0.00	0.00	0.00	.11	.11	.11	0.00	0.00
36 DAMAGED AREA	3.07	4.68	4.18	4.02	3.76	.53	.14	.18	9.15	8.40
37 SEC. CONE 7	.05	.09	0.00	0.00	0.00	.11	.11	.11	0.00	0.00
41 SEC. CONE 9	.05	.09	.09	0.00	0.00	.11	.11	.11	0.00	0.00
42 SEC. DISK 9	.25	.22	.22	.22	.23	.33	.34	.34	.15	.30
43 SEC. CONE 10	2.39	2.32	2.39	2.38	2.45	3.19	2.70	2.60	2.71	3.10
46 STIMULATOR	.08	.04	.03	.03	.02	.11	.00	.00	.15	.15
TOTAL POWER	.151E-10	.651E-11	.397E-11	.358E-11	.279E-11	.305E-13	.570E-14	.670E-15	.922E-23	.933E-24
SOURCE ANG	40.0	45.0	55.0	60.0	75.0	88.0	110.0	120.0	130.0	150.0

Table 13. Percent Table, 2nd 10 angles, 180° azimuth, 22.5μm.

7 SEC. DISK 3	.05	0.00	0.00	0.00	0.00	.09	.23	.34	0.00	0.00
12 LEFT APT.	.94	1.20	.93	.81	.68	1.32	2.15	2.26	.50	.65
14 RIGHT APT.	.29	.44	.29	.23	.18	.43	.91	1.01	0.00	0.00
15 SEC. CONE 4	.05	0.00	0.00	0.00	0.00	.09	.23	.34	0.00	0.00
17 SEC. CONE 5	.02	.06	.07	.08	0.00	.09	.11	.11	0.00	0.00
19 SEC. CONE 1	94.79	93.29	94.07	94.55	94.98	91.58	89.74	89.41	95.14	93.69
20 SEC. APT	.39	1.07	1.01	.85	.72	2.13	2.49	2.48	.17	.97
21 STRUT BACK	.05	.06	.07	.08	.09	.09	.23	.23	0.00	0.00
25 INNER TIP END	.07	.13	0.00	0.00	0.00	.09	.34	.34	0.00	0.00
26 LEFT INNER CONICAL	.02	0.00	0.00	0.00	0.00	0.00	.11	.11	0.00	0.00
32 SECONDARY MIRROR	.00	.00	.00	.00	.00	.00	.00	.00	.01	.01
33 PRIMARY MIRROR	.02	.02	.02	.02	.02	.03	.03	.03	.02	.02
34 SEC. CONE 6	.02	.06	0.00	0.00	0.00	.09	.11	.11	0.00	0.00
36 DAMAGED AREA	.30	.62	.53	.49	.43	.24	.02	.03	.87	.80
37 SEC. CONE 7	.02	.06	0.00	0.00	0.00	.09	.11	.11	0.00	0.00
41 SEC. CONE 9	.02	.06	.07	0.00	0.00	.09	.11	.11	0.00	0.00
42 SEC. DISK 9	.26	.21	.22	.22	.23	.30	.34	.34	.17	.32
43 SEC. CONE 10	2.59	2.61	2.65	2.61	2.62	3.17	2.73	2.64	2.97	3.39
46 STIMULATOR	.10	.09	.07	.06	.04	.13	.00	.00	.17	.16
TOTAL POWER	.310E-10	.916E-11	.524E-11	.455E-11	.327E-11	.304E-13	.565E-14	.670E-15	.198E-21	.201E-2
SOURCE ANG	40.0	45.0	55.0	60.0	75.0	88.0	110.0	120.0	130.0	150.0

Table 14. Percent Table, 2nd 10 angles, 180° azimuth, 64.5μm.

7 SEC. DISK 3	.03	0.00	0.00	0.00	0.00	.06	.23	.33	0.00	0.00
12 LEFT APT.	.64	1.05	.85	.75	.65	1.10	2.14	2.22	.50	.65
14 RIGHT APT.	.24	.34	.23	.19	.16	.31	.90	.99	0.00	0.00
15 SEC. CONE 4	.03	0.00	0.00	0.00	0.00	.06	.23	.33	0.00	0.00
17 SEC. CONE 5	.02	.05	.06	.06	0.00	.06	.11	.11	0.00	0.00
19 SEC. CONE 1	95.33	94.17	94.69	95.05	95.36	92.85	89.81	89.60	95.71	94.21
20 SEC. APT	.26	.83	.81	.70	.63	1.56	2.48	2.42	.17	.97
21 STRUT BACK	.03	.05	.06	.06	.08	.06	.23	.22	0.00	0.00
25 INNER TIP END	.05	.10	0.00	0.00	0.00	.06	.34	.33	0.00	0.00
26 LEFT INNER CONICAL	.02	0.00	0.00	0.00	0.00	0.00	.11	.11	0.00	0.00
32 SECONDARY MIRROR	.00	.00	.00	.00	.00	.00	.00	.00	.00	.00
33 PRIMARY MIRROR	.00	.01	.00	.00	.00	.01	.01	.01	.00	.00
34 SEC. CONE 6	.02	.05	0.00	0.00	0.00	.06	.11	.11	0.00	0.00
36 DAMAGED AREA	.11	.24	.21	.19	.17	.15	.01	.02	.30	.27
37 SEC. CONE 7	.02	.05	0.00	0.00	0.00	.06	.11	.11	0.00	0.00
41 SEC. CONE 9	.02	.05	.06	0.00	0.00	.06	.11	.11	0.00	0.00
42 SEC. DISK 9	.26	.21	.21	.21	.22	.26	.34	.34	.17	.32
43 SEC. CONE 10	2.63	2.71	2.73	2.69	2.67	3.11	2.73	2.65	2.99	3.41
46 STIMULATOR	.11	.11	.09	.08	.06	.14	.00	.01	.17	.16
TOTAL POWER	.458E-10	.118E-10	.651E-11	.555E-11	.379E-11	.349E-13	.568E-14	.688E-15	.788E-21	.804E-2
SOURCE ANG	40.0	45.0	55.0	60.0	75.0	88.0	110.0	120.0	130.0	150.0

Table 15. Percent Table, 2nd 10 angles, 180° azimuth, 102.5μm.

7 SEC. DISK 3	0.00	0.00	0.00	0.00	0.00	0.00	.01	.30	.14	.05
12 LEFT APT.	0.00	0.00	.05	.06	2.16	13.43	30.25	.00	.00	.00
14 RIGHT APT.	0.00	0.00	0.00	0.00	0.00	1.28	21.30	0.00	.00	.00
15 SEC. CONE 4	0.00	0.00	0.00	0.00	0.00	0.00	.02	.34	.15	.05
17 SEC. CONE 5	0.00	0.00	0.00	.01	0.00	0.00	.02	.47	.21	.08
19 SEC. CONE 1	0.00	0.00	0.00	97.23	.07	.06	.13	1.00	.56	.59
20 SEC. APT	0.00	0.00	55.23	1.64	0.00	0.00	.01	.17	.09	0.00
21 STRUT BACK	.01	.03	.03	0.00	.15	.61	0.00	.05	.04	.03
25 INNER TIP END	.77	0.00	0.00	0.00	0.00	0.00	0.00	0.00	0.00	0.00
28 RIGHT INNER CON.	.04	0.00	0.00	0.00	0.00	0.00	0.00	0.00	0.00	0.00
29 RIGHT INNER C END	4.13	0.00	0.00	0.00	0.00	0.00	0.00	0.00	0.00	0.00
30 DAMAGED AREA AZIM	55.11	45.91	17.91	.38	11.00	36.72	0.00	0.00	0.00	0.00
32 SECONDARY MIRROR	20.95	20.32	2.33	.07	.00	.06	.00	.02	.00	.00
33 PRIMARY MIRROR	17.85	30.08	16.85	.53	20.30	47.87	47.51	36.71	43.67	34.69
34 SEC. CONE 6	0.00	0.00	0.00	.01	0.00	.01	.04	.30	.44	.18
37 SEC. CONE 7	0.00	0.00	0.00	.01	0.00	.01	.04	24.27	22.17	25.41
39 SEC. CONE 8	0.00	0.00	0.00	0.00	0.00	0.00	.01	.25	.12	.04
41 SEC. CONE 9	0.00	0.00	0.00	.01	3.47	.01	.04	1.91	.73	.58
42 SEC. DISK 9	0.00	0.00	0.00	.05	2.05	.00	.00	.40	.37	.44
43 SEC. CONE 10	0.00	0.00	0.00	0.00	59.81	.00	.02	32.32	30.91	37.95
46 STIMULATOR	1.14	3.67	1.60	0.00	0.00	0.00	0.00	0.00	.00	.00
TOTAL POWER	.200E-04	.649E-05	.904E-05	.153E-03	.169E-05	.241E-06	.591E-07	.369E-08	.384E-08	.276E-08
SOURCE ANG	1.0	2.0	3.0	5.0	10.0	15.0	20.0	25.0	30.0	35.0

Table 16. Percent Table, 1st 10 angles, 90^0 azimuth, 11.5μm.

7 SEC. DISK 3	0.00	0.00	0.00	0.00	0.00	0.00	.02	.45	.23	.08
12 LEFT APT.	0.00	0.00	.10	.06	3.02	51.69	54.49	.00	.00	.00
14 RIGHT APT.	0.00	0.00	0.00	0.00	0.00	4.94	37.63	0.00	.00	.00
15 SEC. CONE 4	0.00	0.00	0.00	0.00	0.00	0.00	.04	.51	.26	.09
17 SEC. CONE 5	0.00	0.00	0.00	.01	0.00	0.00	.04	.70	.34	.11
19 SEC. CONE 1	0.00	0.00	0.00	98.07	.19	.39	.32	3.46	1.93	1.10
20 SEC. APT	0.00	0.00	88.56	1.65	0.00	0.00	.02	.25	.15	0.00
21 STRUT BACK	.05	.18	.05	0.00	.21	2.37	0.00	.08	.06	.04
25 INNER TIP END	3.93	0.00	0.00	0.00	0.00	0.00	0.00	0.00	0.00	0.00
28 RIGHT INNER CON.	.19	0.00	0.00	0.00	0.00	0.00	0.00	0.00	0.00	0.00
29 RIGHT INNER C END	21.23	0.00	0.00	0.00	0.00	0.00	0.00	0.00	0.00	0.00
30 DAMAGED AREA AZIM	49.57	48.88	5.03	.07	2.93	24.74	0.00	0.00	0.00	0.00
32 SECONDARY MIRROR	11.31	12.98	1.40	.01	.00	.00	.00	.00	.00	.00
33 PRIMARY MIRROR	7.84	15.65	2.31	.05	2.42	15.76	7.18	4.70	6.20	4.33
34 SEC. CONE 6	0.00	0.00	0.00	.01	0.00	.03	.07	1.34	.72	.26
37 SEC. CONE 7	0.00	0.00	0.00	.01	0.00	.03	.07	37.36	36.79	37.13
39 SEC. CONE 8	0.00	0.00	0.00	0.00	0.00	0.00	.02	.37	.19	.06
41 SEC. CONE 9	0.00	0.00	0.00	.01	4.84	.03	.07	1.81	1.21	.85
42 SEC. DISK 9	0.00	0.00	0.00	.05	2.87	.00	.00	.61	.62	.64
43 SEC. CONE 10	0.00	0.00	0.00	0.00	83.52	.01	.04	48.36	51.29	55.31
46 STIMULATOR	5.88	22.31	2.56	0.00	0.00	0.00	0.00	0.00	.00	.00
TOTAL POWER	.388E-05	.107E-05	.501E-05	.152E-03	.106E-05	.627E-07	.334E-07	.233E-08	.232E-08	.188E-08
SOURCE ANG	1.0	2.0	3.0	5.0	10.0	15.0	20.0	25.0	30.0	35.0

Table 17. Percent Table, 1st 10 angles, 90^0azimuth, 22.5μm.

7 SEC. DISK 3	0.00	0.00	0.00	0.00	0.00	0.00	.02	.46	.25	.08
12 LEFT APT.	0.00	0.00	.10	.06	3.17	82.29	58.32	.01	.01	.01
14 RIGHT APT.	0.00	0.00	0.00	0.00	0.00	7.86	40.27	0.00	.00	.00
15 SEC. CONE 4	0.00	0.00	0.00	0.00	0.00	0.00	.04	.52	.27	.10
17 SEC. CONE 5	0.00	0.00	0.00	.01	0.00	0.00	.04	.72	.36	.12
19 SEC. CONE 1	0.00	0.00	0.00	98.19	.56	1.66	.75	5.94	3.34	2.10
20 SEC. APT	0.00	0.00	96.44	1.66	0.00	0.00	.02	.26	.16	0.00
21 STRUT BACK	.13	.64	.05	0.00	.22	3.77	0.00	.08	.07	.04
25 INNER TIP END	10.83	0.00	0.00	0.00	0.00	0.00	0.00	0.00	0.00	0.00
28 RIGHT INNER CON.	.52	0.00	0.00	0.00	0.00	0.00	0.00	0.00	0.00	0.00
29 RIGHT INNER C END	58.47	0.00	0.00	0.00	0.00	0.00	0.00	0.00	0.00	0.00
30 DAMAGED AREA AZIM	11.86	15.28	.48	.01	.27	3.42	0.00	0.00	0.00	0.00
32 SECONDARY MIRROR	1.32	1.98	.06	.00	.00	.00	.00	.00	.00	.00
33 PRIMARY MIRROR	.69	1.79	.08	.00	.08	.80	.24	.15	.21	.14
34 SEC. CONE 6	0.00	0.00	0.00	.01	0.00	.06	.08	1.37	.76	.27
37 SEC. CONE 7	0.00	0.00	0.00	.01	0.00	.06	.08	38.17	38.60	38.37
39 SEC. CONE 8	0.00	0.00	0.00	0.00	0.00	0.00	.02	.38	.20	.06
41 SEC. CONE 9	0.00	0.00	0.00	.01	5.08	.06	.08	1.85	1.27	.97
42 SEC. DISK 9	0.00	0.00	0.00	.05	3.01	.00	.00	.63	.65	.66
43 SEC. CONE 10	0.00	0.00	0.00	0.00	87.61	.04	.05	49.48	53.86	57.18
46 STIMULATOR	16.18	80.31	2.79	0.00	0.00	0.00	0.00	0.00	.00	.00
TOTAL POWER	.141E-05	.296E-06	.460E-05	.152E-03	.101E-05	.394E-07	.312E-07	.228E-08	.221E-08	.182E-08
SOURCE ANG	1.0	2.0	3.0	5.0	10.0	15.0	20.0	25.0	30.0	35.0

Table 18. Percent Table, 1st 10 angles, 90° azimuth, 64.5μm.

7 SEC. DISK 3	0.00	0.00	0.00	0.00	0.00	0.00	.02	.45	.24	.08
12 LEFT APT.	0.00	0.00	.10	.06	3.16	83.89	58.22	.02	.01	.01
14 RIGHT APT.	0.00	0.00	0.00	0.00	0.00	8.02	40.20	0.00	.00	.00
15 SEC. CONE 4	0.00	0.00	0.00	0.00	0.00	0.00	.04	.51	.27	.10
17 SEC. CONE 5	0.00	0.00	0.00	.01	0.00	0.00	.04	.70	.35	.12
19 SEC. CONE 1	0.00	0.00	0.00	98.19	.90	2.65	1.10	7.94	4.48	2.94
20 SEC. APT	0.00	0.00	96.85	1.56	0.00	0.00	.02	.25	.15	0.00
21 STRUT BACK	.14	.73	.05	0.00	.22	3.84	0.00	.08	.07	.04
25 INNER TIP END	11.95	0.00	0.00	0.00	0.00	0.00	0.00	0.00	0.00	0.00
28 RIGHT INNER CON.	.58	0.00	0.00	0.00	0.00	0.00	0.00	0.00	0.00	0.00
29 RIGHT INNER C END	64.48	0.00	0.00	0.00	0.00	0.00	0.00	0.00	0.00	0.00
30 DAMAGED AREA AZIM	4.47	6.00	.16	.00	.09	1.19	0.00	0.00	0.00	0.00
32 SECONDARY MIRROR	.35	.57	.02	.00	.00	.00	.00	.00	.00	.00
33 PRIMARY MIRROR	.17	.45	.02	.00	.02	.18	.05	.03	.04	.03
34 SEC. CONE 6	0.00	0.00	0.00	.01	0.00	.06	.08	1.34	.75	.27
37 SEC. CONE 7	0.00	0.00	0.00	.01	0.00	.06	.08	37.38	38.19	38.07
39 SEC. CONE 8	0.00	0.00	0.00	0.00	0.00	0.00	.02	.37	.20	.06
41 SEC. CONE 9	0.00	0.00	0.00	.01	5.08	.06	.08	1.81	1.26	.87
42 SEC. DISK 9	0.00	0.00	0.00	.05	3.00	.00	.00	.62	.65	.66
43 SEC. CONE 10	0.00	0.00	0.00	0.00	87.53	.06	.06	48.51	53.32	56.76
46 STIMULATOR	17.85	92.25	2.80	0.00	0.00	0.00	0.00	0.00	.00	.00
TOTAL POWER	.128E-05	.258E-06	.459E-05	.152E-03	.101E-05	.386E-07	.313E-07	.233E-08	.223E-08	.183E-08
SOURCE ANG	1.0	2.0	3.0	5.0	10.0	15.0	20.0	25.0	30.0	35.0

Table 19. Percent Table, 1st 10 angles, 90° azimuth, 102.5μm.

SEC. DISK 3	.00	0.00	.01	.01	.00	.00
LEFT APT.	.01	.01	.19	.15	.07	.02
RIGHT APT.	.01	.00	.07	.06	.03	.01
SEC. CONE 4	.00	0.00	.01	.01	.00	.00
SEC. CONE 5	.00	.00	.01	.01	.00	.00
SEC. CONE 1	.90	.90	30.20	29.01	11.46	1.30
SEC. APT	0.00	0.00	1.19	1.09	.50	.10
STRUT BACK	.00	.00	.02	.02	.00	.00
INNER TIP END	.00	.00	0.00	0.00	0.00	.00
LEFT INNER CONICAL	20.28	19.40	5.74	5.34	14.65	19.99
MIDDLE INNER CON.	77.51	78.29	13.37	14.06	53.10	75.75
SECONDARY MIRROR	.70	.90	28.22	28.02	11.46	1.10
PRIMARY MIRROR	.50	.50	20.30	21.09	8.47	.70
SEC. CONE 6	.00	.00	.01	.01	.00	.00
DAMAGED AREA	.09	.09	.17	.15	.06	.01
SEC. CONE 7	.00	.00	0.00	0.00	0.00	0.00
SEC. CONE 9	.00	.00	.01	.01	.00	.00
SEC. DISK 9	.00	.00	.04	.04	.02	.00
SEC. CONE 10	.01	.01	.43	.42	.17	.02
STIMULATOR	0.00	0.00	.01	.01	.00	0.00
TOTAL POWER	.702E-09	.692E-09	.117E-11	.925E-11	.855E-13	.241E-13
SOURCE ANG	40.0	45.0	55.0	60.0	75.0	88.0

Table 20. Percent Table, 2nd 10 angles, 90° azimuth, visible.

7 SEC. DISK 3	.11	0.00	.10	.10	.10	.30	.10	.10	.10	0.00
12 LEFT APT.	1.22	1.26	2.53	2.21	1.50	2.10	1.10	1.00	.90	.60
14 RIGHT APT.	.49	.56	.98	.79	.60	.90	.20	.20	.20	.10
15 SEC. CONE 4	.11	0.00	.10	.10	.10	.30	.10	.10	.10	0.00
17 SEC. CONE 5	.06	.08	.18	.17	.10	.10	.10	.10	.10	.10
19 SEC. CONE 1	73.27	69.24	65.76	66.34	79.08	79.88	71.30	71.90	74.33	79.72
20 SEC. APT	.96	1.36	0.00	0.00	0.00	0.00	0.00	0.00	0.00	0.00
21 STRUT BACK	.11	.08	.25	.25	.10	.20	.10	.10	.10	.10
25 INNER TIP END	.17	.16	.03	.03	0.00	.30	0.00	0.00	0.00	0.00
26 LEFT INNER CONICAL	.06	0.00	0.00	0.00	0.00	.10	0.00	0.00	0.00	0.00
32 SECONDARY MIRROR	.49	.56	2.08	2.16	1.10	.60	1.80	1.90	1.60	1.20
33 PRIMARY MIRROR	7.33	7.49	17.45	16.36	11.41	11.51	13.20	13.50	11.59	9.59
34 SEC. CONE 6	.06	.08	.10	.10	.10	.10	.10	.10	.10	.10
36 DAMAGED AREA	13.37	16.99	2.15	2.05	1.40	.80	5.50	4.70	5.29	6.29
37 SEC. CONE 7	.06	.08	.03	.03	.00	.00	.10	.10	.10	.10
41 SEC. CONE 9	.06	.08	.18	.10	.10	.10	.10	.10	.10	.10
42 SEC. DISK 9	.20	.18	.63	.62	.40	.30	.40	.40	.40	.30
43 SEC. CONE 10	1.88	1.78	7.43	7.77	3.80	2.41	5.60	5.40	4.90	3.69
46 STIMULATOR	.04	.02	.15	.23	.10	.00	.20	.20	.10	.10
TOTAL POWER	.129E-10	.717E-11	.100E-11	.739E-12	.378E-14	.186E-15	.874E-25	.108E-24	.123E-24	.136E-24
SOURCE ANG	40.0	45.0	55.0	60.0	75.0	88.0	110.0	120.0	130.0	150.0

Table 21. Percent Table, 2nd 10 angles, 90° azimuth, 11.5μm.

7 SEC. DISK 3	.09	0.00	.12	.12	.11	.34	.12	.12	.12	0.00
12 LEFT APT.	1.23	1.45	2.72	2.37	1.72	2.38	1.35	1.22	1.08	.70
14 RIGHT APT.	.45	.62	.90	.80	.69	1.02	.24	.24	.24	.12
15 SEC. CONE 4	.09	0.00	.12	.12	.11	.34	.12	.12	.12	0.00
17 SEC. CONE 5	.05	.09	.19	.19	.11	.11	.12	.12	.12	.12
19 SEC. CONE 1	90.32	87.69	82.60	82.97	90.46	90.47	87.19	87.48	88.90	91.67
20 SEC. APT	.80	1.50	0.00	0.00	0.00	0.00	0.00	0.00	0.00	0.00
21 STRUT BACK	.09	.09	.27	.26	.11	.23	.12	.12	.12	.12
25 INNER TIP END	.14	.18	.05	.05	0.00	.34	0.00	0.00	0.00	0.00
26 LEFT INNER CONICAL	.05	0.00	0.00	0.00	0.00	.11	0.00	0.00	0.00	0.00
32 SECONDARY MIRROR	.07	.08	.28	.28	.13	.07	.23	.24	.20	.12
33 PRIMARY MIRROR	.69	.78	1.57	1.46	1.12	1.12	1.38	1.41	1.19	.86
34 SEC. CONE 6	.05	.09	.12	.12	.11	.11	.12	.12	.12	.12
36 DAMAGED AREA	3.07	4.68	.39	.36	.28	.16	1.18	1.00	1.11	1.28
37 SEC. CONE 7	.05	.09	.05	.05	.00	.00	.12	.12	.12	.12
41 SEC. CONE 9	.05	.09	.19	.12	.11	.11	.17	.12	.12	.12
42 SEC. DISK 9	.25	.22	.70	.69	.46	.34	.49	.49	.48	.35
43 SEC. CONE 10	2.39	2.32	9.50	9.74	4.35	2.75	6.85	6.82	5.86	4.19
46 STIMULATOR	.08	.04	.22	.29	.11	.00	.24	.24	.12	.12
TOTAL POWER	.151E-10	.651E-11	.103E-11	.774E-12	.330E-14	.165E-15	.535E-24	.664E-24	.771E-24	.876E-2
SOURCE ANG	40.0	45.0	55.0	60.0	75.0	88.0	110.0	120.0	130.0	150.0

Table 22. Percent Table, 2nd 10 angles, 90° azimuth, 22.5μm.

7 SEC. DISK 3	.05	0.00	.12	.12	.12	.34	.13	.12	.12	0.00
12 LEFT APT.	.94	1.20	2.07	1.86	1.74	2.40	1.38	1.25	1.10	.71
14 RIGHT APT.	.29	.44	.60	.54	.70	1.01	.25	.25	.24	.12
15 SEC. CONE 4	.05	0.00	.12	.12	.12	.34	.13	.12	.12	0.00
17 SEC. CONE 5	.02	.06	.16	.16	.17	.12	.13	.12	.12	.12
19 SEC. CONE 1	94.79	93.29	85.30	85.45	91.80	91.47	89.54	89.73	91.04	93.67
20 SEC. APT	.39	1.07	0.00	0.00	0.00	0.00	0.00	0.00	0.00	0.00
21 STRUT BACK	.05	.06	.20	.19	.12	.23	.13	.12	.12	.12
25 INNER TIP END	.07	.13	.08	.09	0.00	.33	0.00	0.00	0.00	0.00
26 LEFT INNER CONICAL	.02	0.00	0.00	0.00	0.00	.11	0.00	0.00	0.00	0.00
32 SECONDARY MIRROR	.00	.00	.01	.01	.01	.00	.01	.01	.01	.01
33 PRIMARY MIRROR	.02	.02	.04	.03	.04	.04	.05	.05	.04	.03
34 SEC. CONE 6	.02	.06	.12	.12	.12	.12	.13	.12	.12	.12
36 DAMAGED AREA	.30	.62	.02	.02	.02	.02	.10	.09	.10	.11
37 SEC. CONE 7	.02	.06	.08	.08	.00	.00	.13	.12	.12	.12
41 SEC. CONE 9	.02	.06	.16	.12	.12	.12	.13	.12	.12	.12
42 SEC. DISK 9	.26	.21	.59	.58	.46	.36	.50	.50	.49	.36
43 SEC. CONE 10	2.59	2.61	10.08	10.22	4.42	3.00	.03	.7.00	6.00	4.28
46 STIMULATOR	.10	.09	.27	.31	.12	.01	.25	.25	.12	.12
TOTAL POWER	.310E-10	.916E-11	.184E-11	.141E-11	.325E-14	.163E-15	.123E-22	.153E-22	.177E-22	.202E-22
SOURCE ANG	40.0	45.0	55.0	60.0	75.0	88.0	110.0	120.0	130.0	150.0

Table 23. Percent Table, 2nd 10 angles, 90° azimuth, 64.5 μm.

7	SEC. DISK 3	.03	0.00	.12	.11	.12	.33	.13	.13	.12	0.00
12	LEFT APT.	.84	1.06	1.62	1.67	1.74	2.39	1.38	1.25	1.10	.71
14	RIGHT APT.	.24	.34	.49	.45	.70	.99	.25	.25	.25	.13
15	SEC. CONE 4	.03	0.00	.12	.11	.12	.33	.13	.13	.12	0.00
17	SEC. CONE 5	.02	.05	.14	.14	.12	.13	.13	.13	.12	.12
19	SEC. CONE 1	95.42	94.37	85.65	95.76	91.84	91.22	89.67	89.85	91.16	93.80
20	SEC. APT	.26	.13	0.00	0.00	0.00	0.00	0.00	0.00	0.00	0.00
21	SNOUT BACK	.03	.05	.17	.17	.12	.22	.13	.13	.12	.12
25	INNER TIP END	.05	.00	.09	.09	0.00	.32	0.00	0.00	0.00	0.00
26	LEFT INNER CONICAL	.02	0.00	0.00	0.00	0.00	.11	0.00	0.00	0.00	0.00
32	SECONDARY MIRROR	.00	.00	.00	.00	.00	.00	.00	.00	.00	.00
33	PRIMARY MIRROR	.00	.01	.01	.01	.01	.01	.01	.01	.01	.01
34	SEC. CONE 6	.02	.05	.12	.11	.12	.12	.13	.13	.12	.12
36	DAMAGED AREA	.01	.02	.00	.00	.00	.00	.00	.00	.00	.00
37	SEC. CONE 7	.02	.05	.09	.09	.00	.01	.13	.13	.12	.12
41	SEC. CONE 9	.02	.05	.14	.11	.12	.12	.13	.13	.12	.12
42	SEC. DISK 9	.26	.21	.55	.54	.47	.38	.50	.50	.49	.36
43	SEC. CONE 10	2.63	2.71	10.21	10.31	4.43	3.34	7.04	7.01	6.00	4.29
46	STIMULATOR	.11	.11	.29	.32	.12	.12	.25	.25	.12	.12
	TOTAL POWER	.459E-10	.118E-10	.260E-11	.199E-11	.325E-14	.165E-15	.492E-22	.611E-22	.711E-22	.809E-22
	SOURCE ANG	40.0	45.0	55.0	60.0	75.0	98.0	110.0	120.0	130.0	150.0

Table 24. Percent Table, 2nd 10 angles, 90° azimuth, 102.5μm.

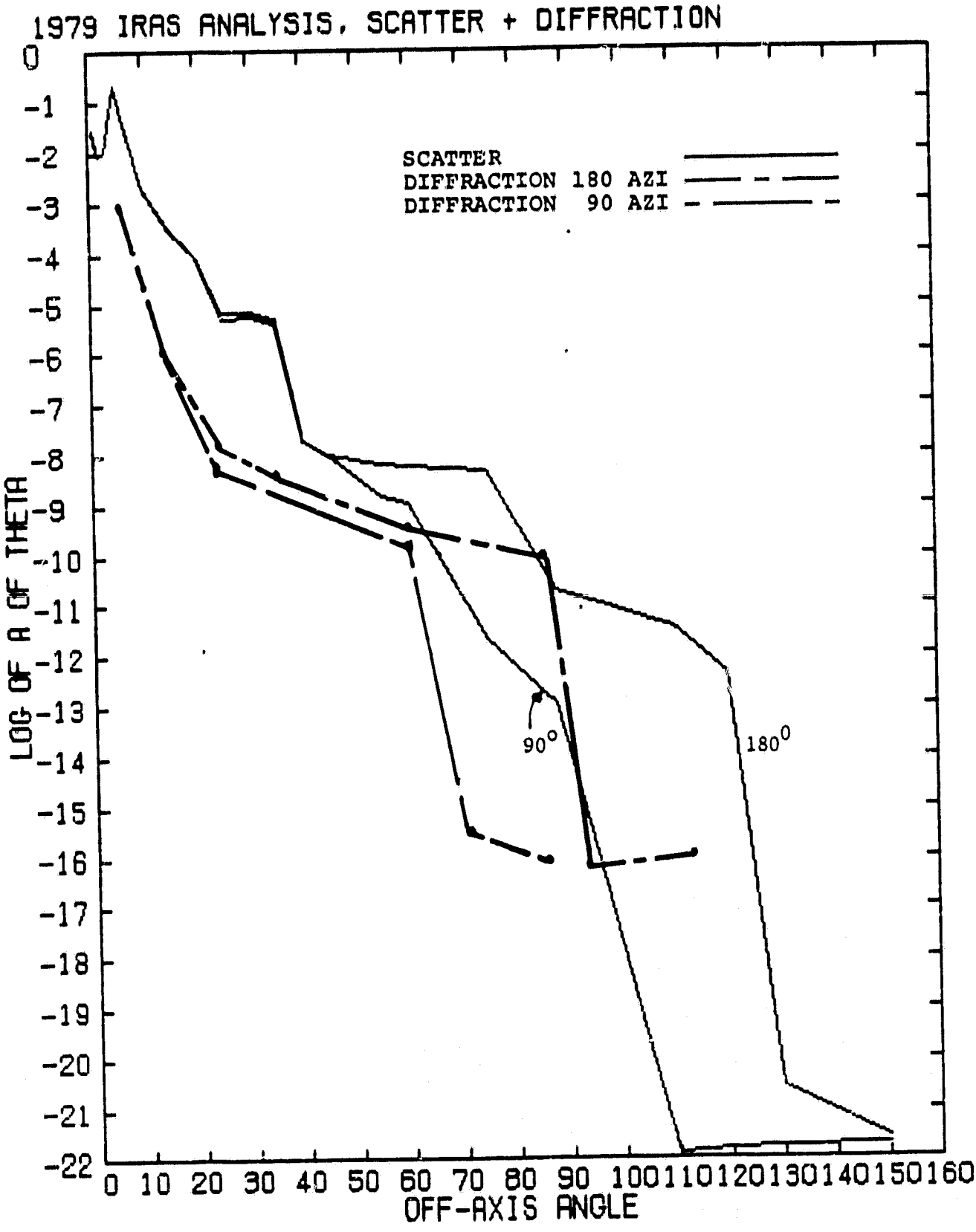

Figure 9. A(θ) for 8 - 15 μm. band.

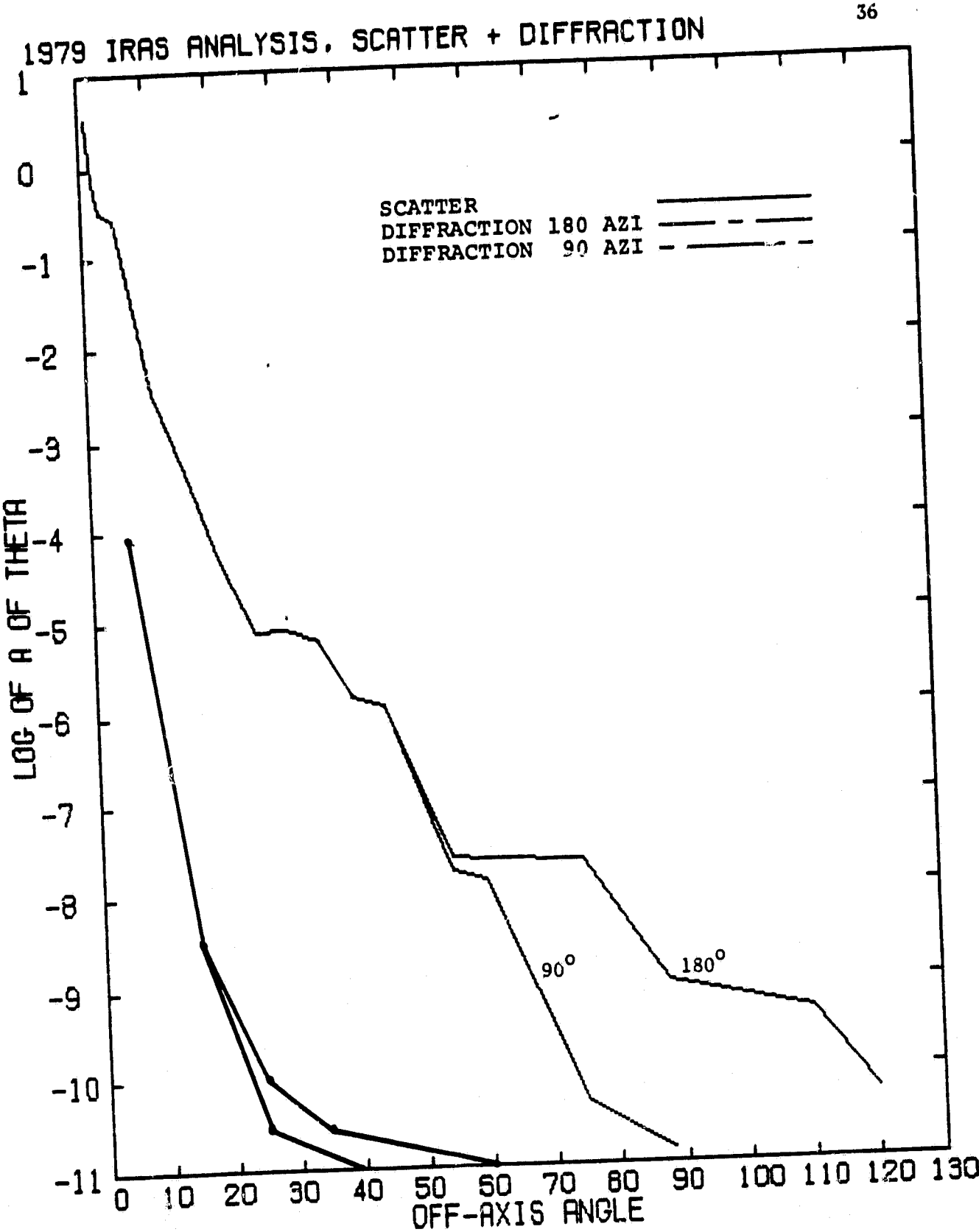

Figure 10. A(Θ) for visible.

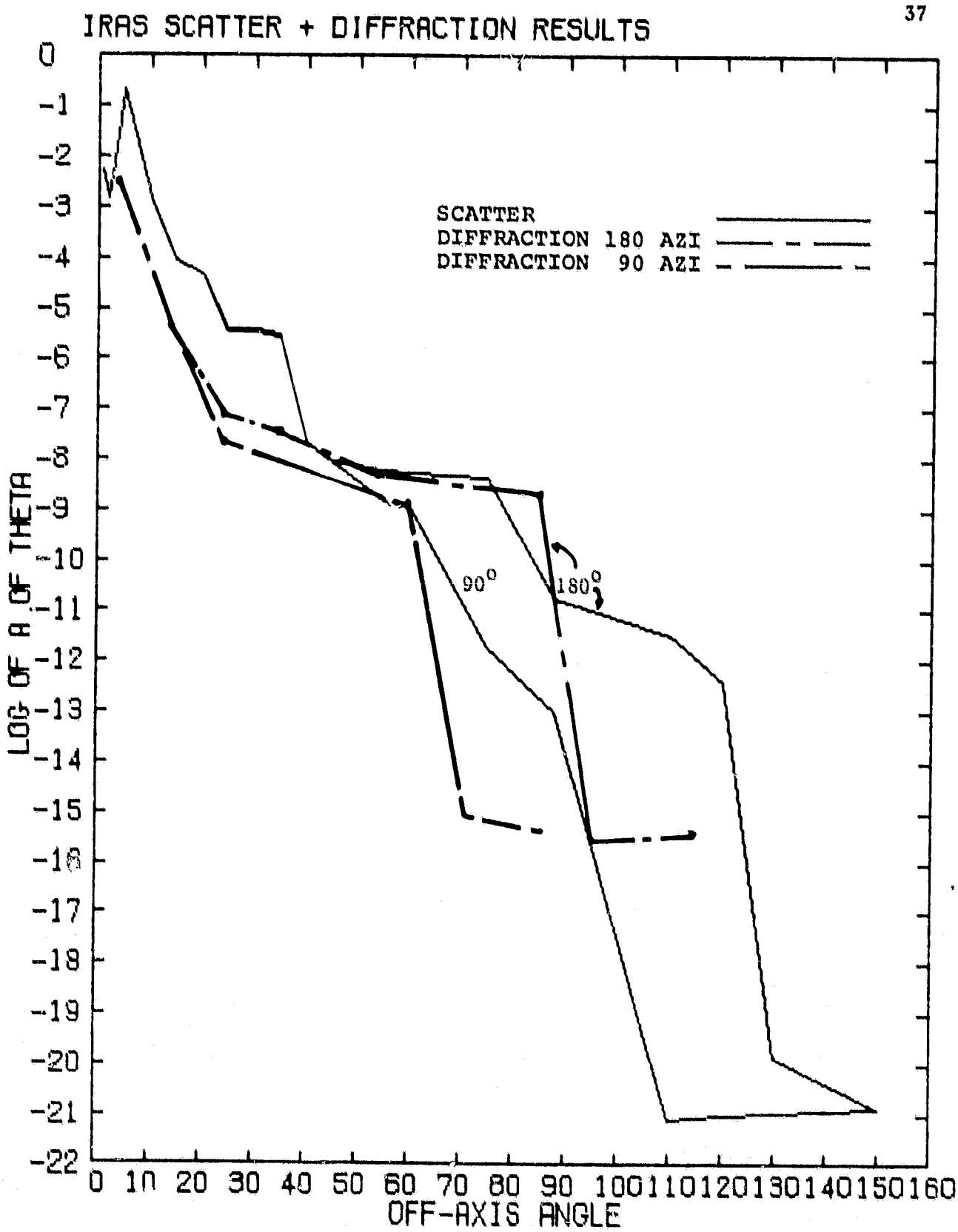

Figure 11. A(θ) for 15 to 30 μm. band.

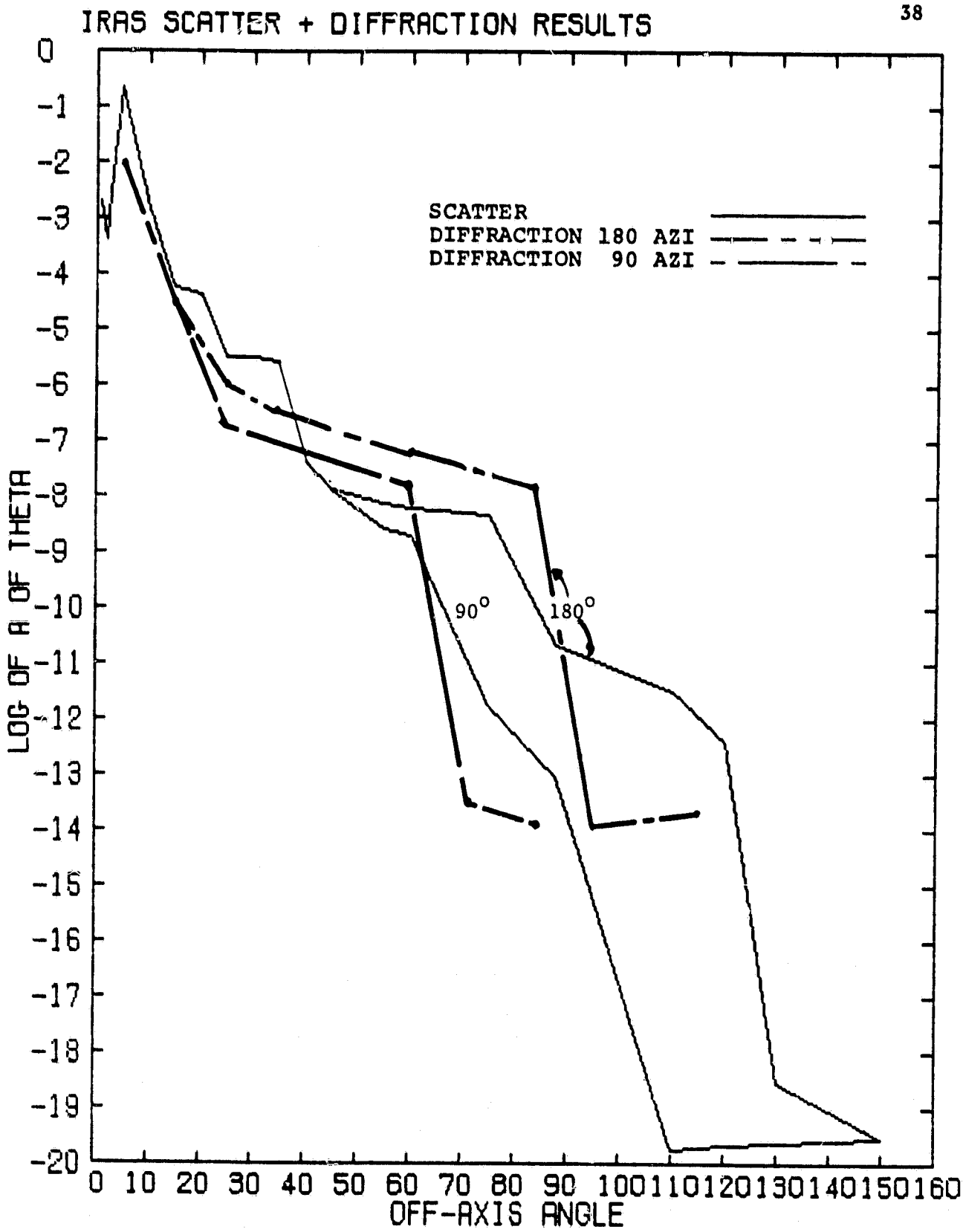

Figure 12. A(Θ) for 48 to 81 μm. band.

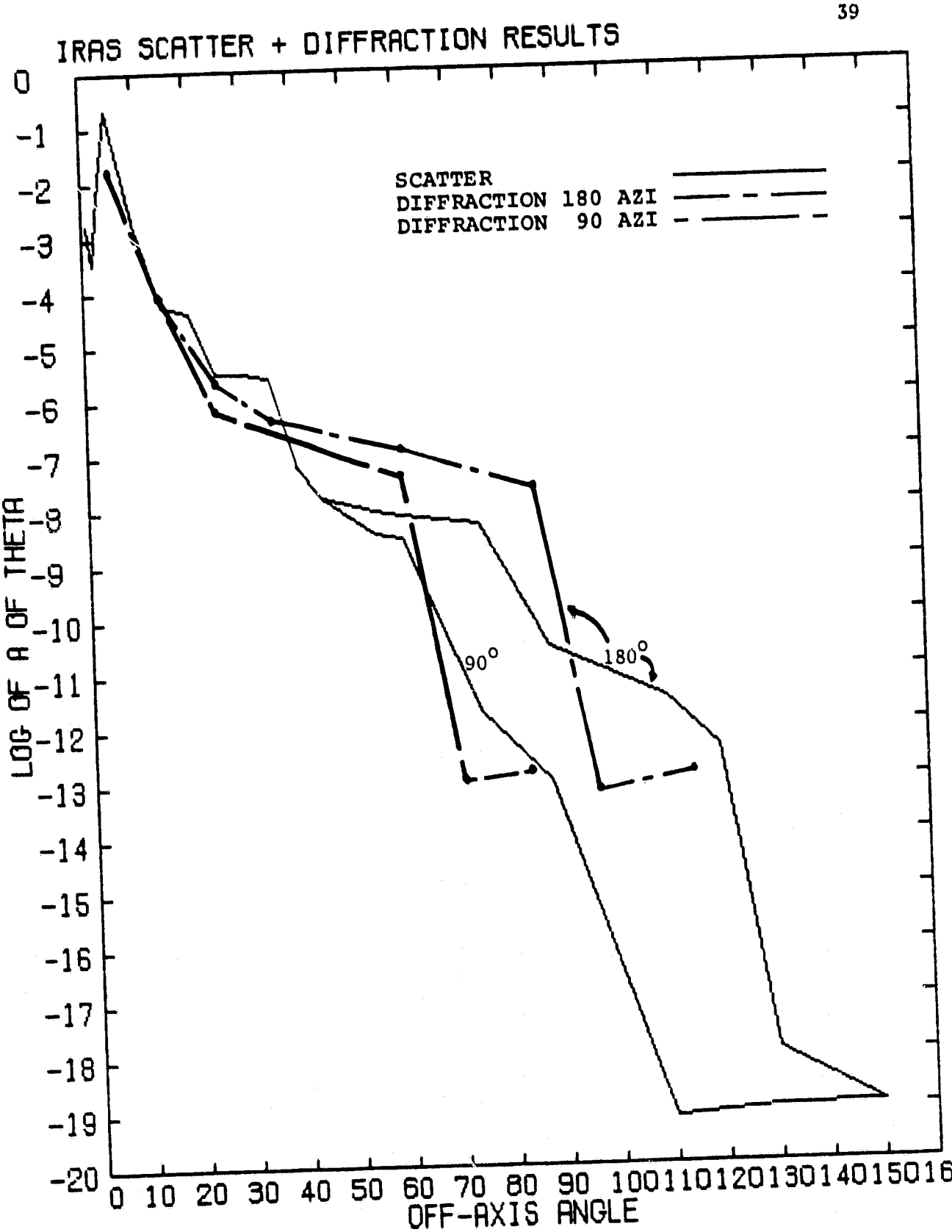

Figure 13. A(Θ) for 87 to 118 μm. band.

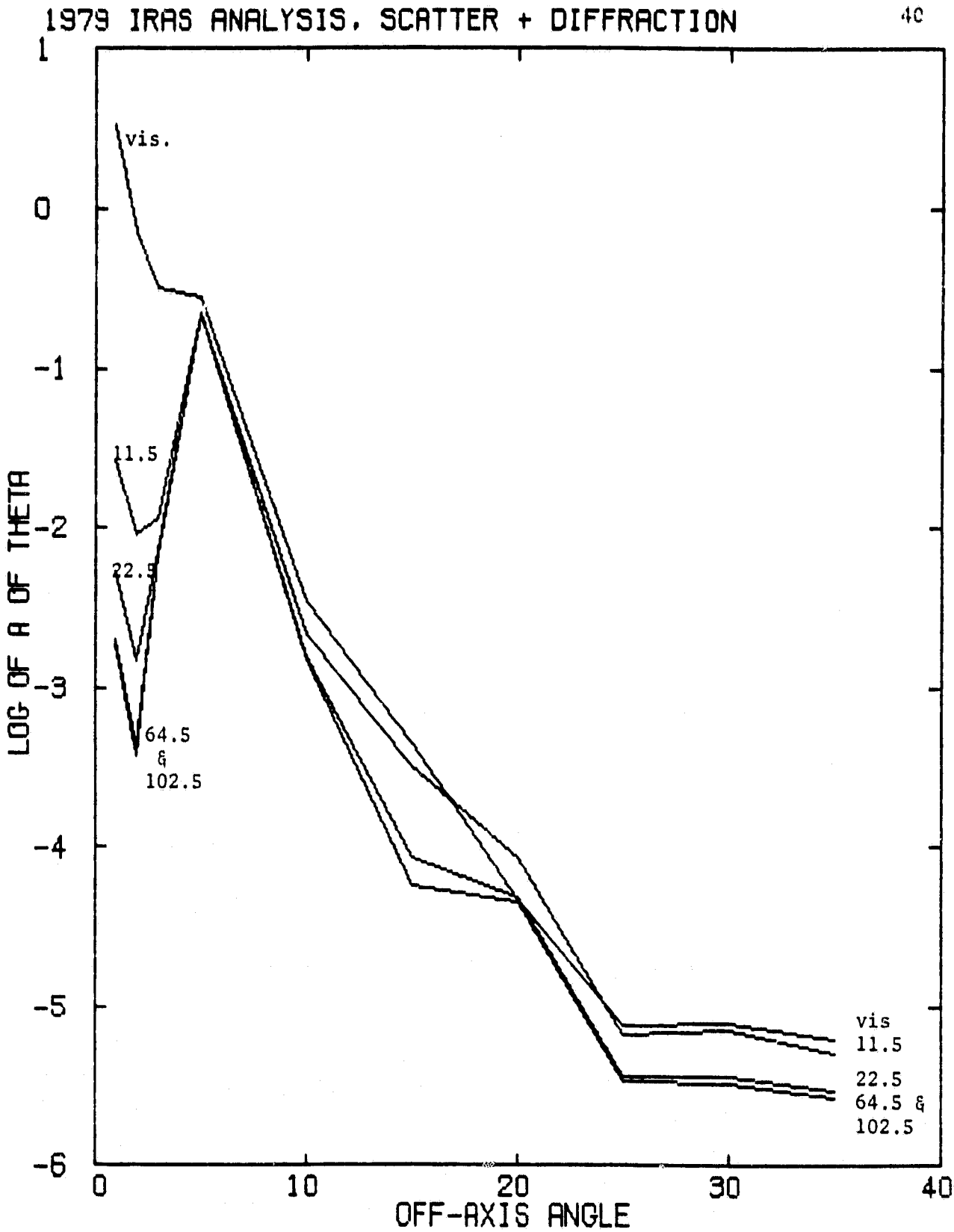

Figure 14. Overplot of all wavebands for 180°, first 10 angles.

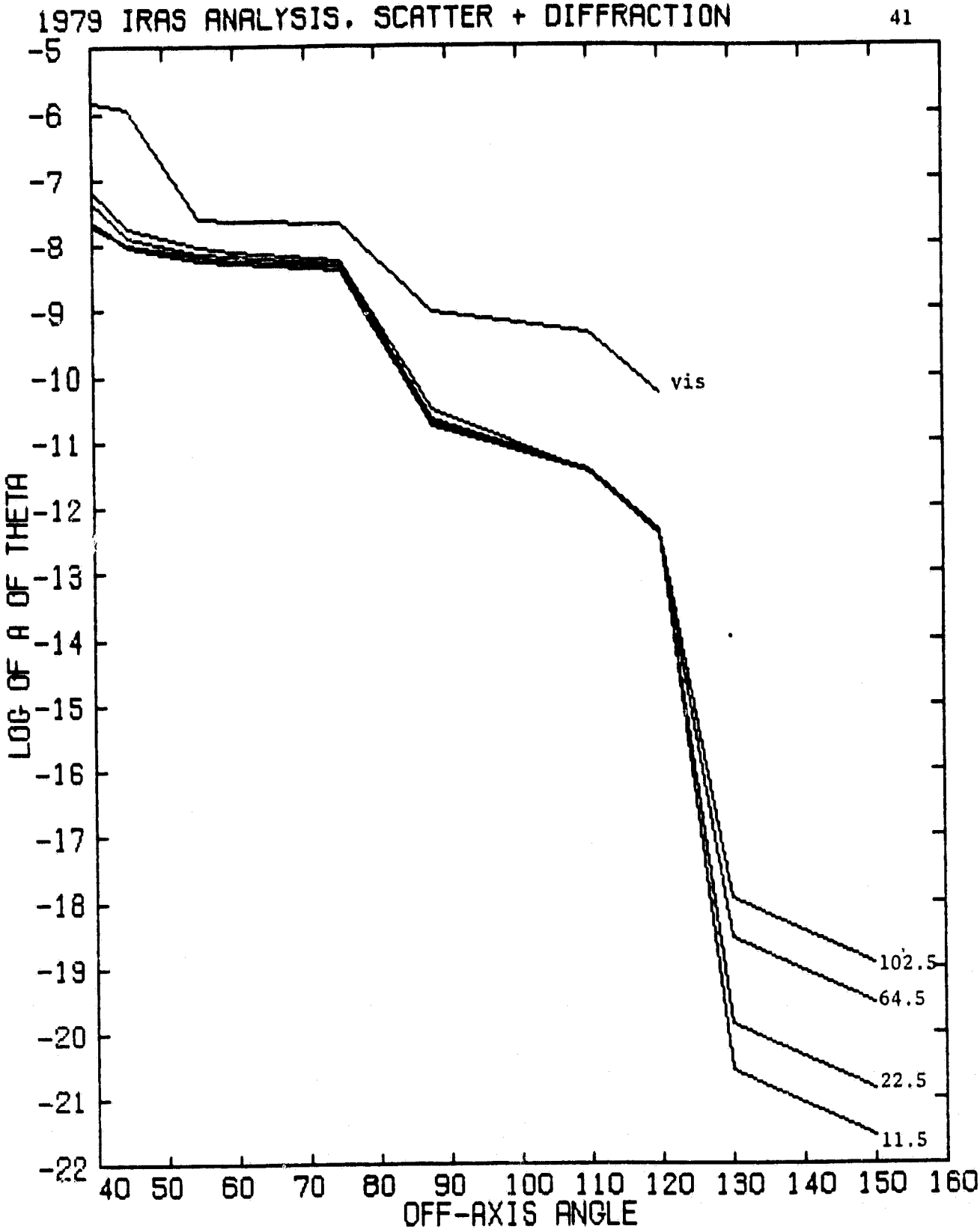

Figure 15. Overplot of all wavebands for 180°, second 10 angles.

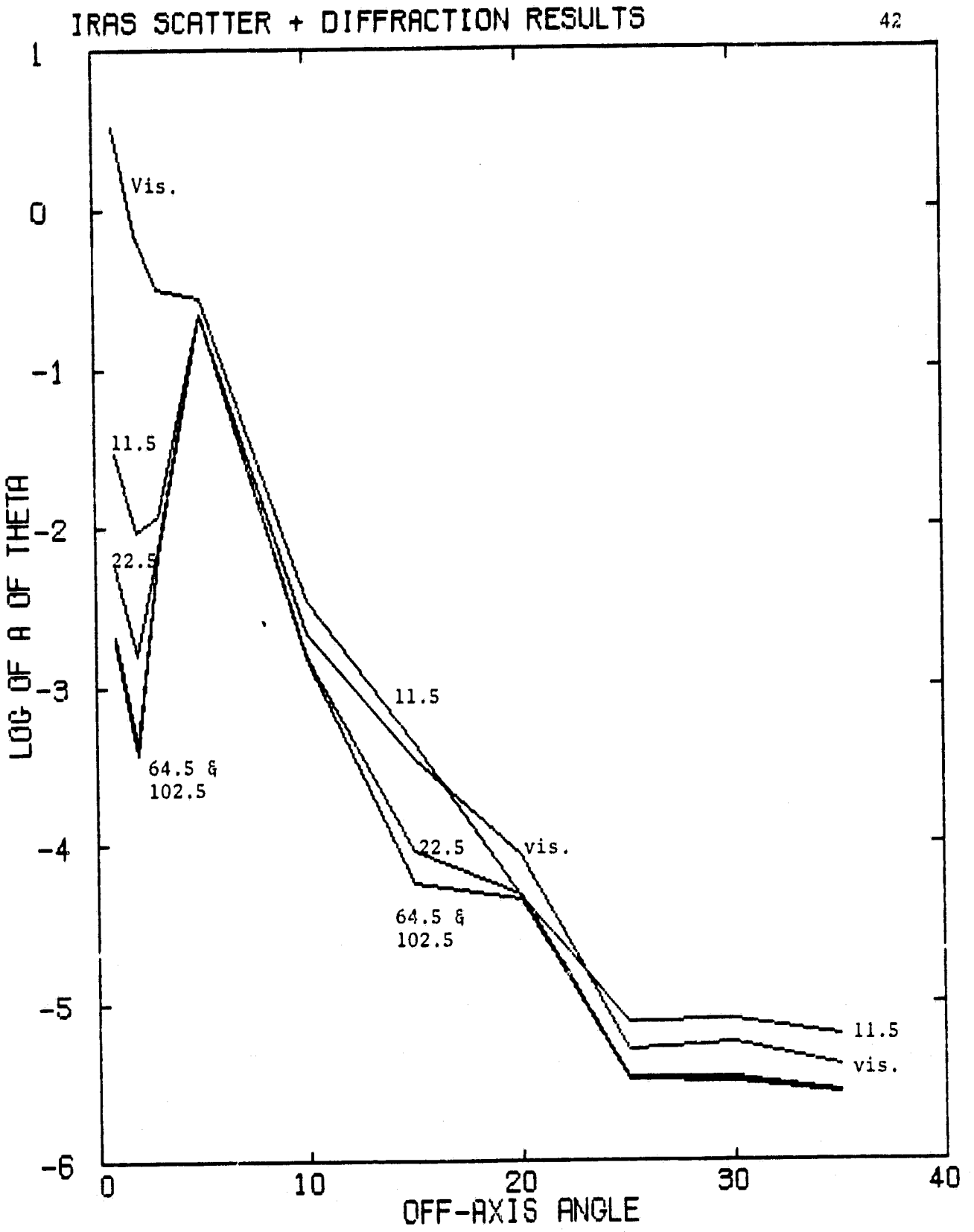

Figure 16. Overplot of all wavebands for 90° azimuth - 1st 10 angles.

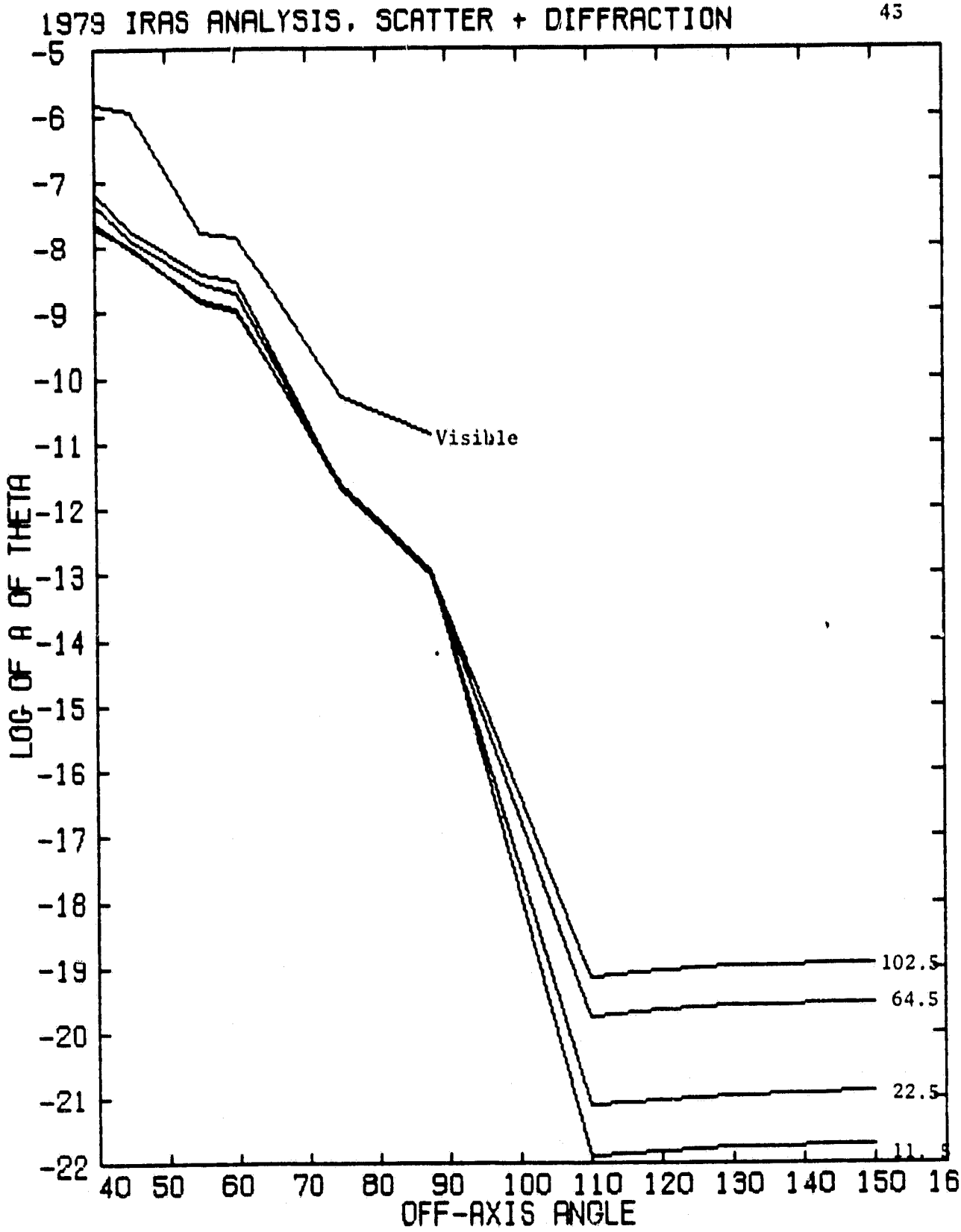

Figure 17. Overplot of all wavebands for 90° azimuth - 2nd 10 angles.

Discussion

The mirrors dominate the stray light contributors for 11.5μ up to 35^{o} with a peak at 5^{o} due to the forward scattering off object 18 and another smaller peak at 20^{o} because of the aperture stop. Beyond 35^{o} the secondary baffle dominates, with object 19 taking the most blame. At longer wavelengths the mirrors, as expected, decrease in importance with a corresponding increase in importance of the black surfaces. The visible wavelengths find the stray light dominated by forward scatter off the inner conical baffle at angles larger than 35^{o} and by mirror scatter at smaller angles. The peaks at 5^{o} and 20^{o} seem to disappear with the visible wavelengths because of the increased importance of the mirror scatter which has a smooth falloff.

In the 90^{o} azimuth the contributors remain essentially the same, although the manner in which the power reaches the critical objects changes due to the altered sunshade obscuration.

A few major drops in the $A(\theta)$ curve signify the change in scattering levels needed for power to reach the image. Up to 20^{o} the critical objects receive direct power for level one scattering. From 25^{o} to 35^{o} object 8 is illuminated but it has no baffle vanes as does the also illuminated objects 5 and 6, so the drop off at this point is not large. (The large forward scattering of Martin Black puts a lot of power on the critical objects because there are no vanes to block it.) Another drop occurs at 88^{o}, where objects 5 and 6 are no longer illuminated; instead, only object 2 is illuminated and diffraction transfers remain, increasing the scattering levels from

two to three. Finally, at 121° the sunshade is no longer illuminated, leaving only diffraction at level four stray light. The same progression occurs at the 90° azimuth only at smaller angles.

Comparison with Requirements

For simplicity the required A(θ) was not plotted in the A(θ) plots, instead the ratio of required to expected A(θ) is presented in Table 25 for an azimuth of 180°.

Table 25. Required to expected A(θ)

θ	Spectral Band (μm) 0.4-0.9	8-15	15-30	48-81	87-118
5°	35.7	31.25	1.35	0.18	0.090
24°	$3.9 \times 10^{+4}$	1.5	2.17	1.19	1.46
60°	13.0	8.52	19.12	30.08	11.35
88°	103.5	1036.	503.	180.0	131.6

Most of the ratios are greater than one by a good deal, with the exception of the 5° case at the two long infrared wavelengths, and this is due to the high forward scatter from object 19 just at that angle.

Scatter and Diffraction Comparison

One bit of information the percent tables do not show is what fraction of the energy reaching the detectors is due to scatter and diffraction. The ratio of scatter to diffraction was calculated for the wavelength of 11.5μ and 102.5μ (the center of the 8-15μ band and the 87-118μ band) and for angles of 10° to 120°. Diffraction was not calculated for 5° and under, while scatter was not calculated for

angles larger than 120°. The results (Table 26) indicate that scatter is dominant at 11.5μ for all angles, while diffraction dominates for intermediate angles at 102.5μ.

Table 26. Scatter to diffraction ratio.

	Source Angle									
λ	10	15	20	25	30	35	40	45	55	60
11.5	1300	1100	1300	220	460	550	1.2	4	5.7	6.9
102.5	151	127	143	125	52	62	.14	.45	.64	.77

λ	75	88	110	120
11.5	11	65	5400	1300
102.5	1.3	.82	68	17

The significance of Table 26 is that it shows what improvement is possible by changing scattering characteristics of the surfaces. The diffraction contribution is fixed with the geometry, so only the scatter can decrease with improved coatings, but diffraction will still be present no matter how perfect the coatings are. Recall also that the diffraction contribution is for one vane only and probably is much higher when the other vane tips are considered.

Thermal Emission Results

The percent table for the objects scattering the thermally emitted radiation to the detector is shown in Table 27.

Table 27. Percent table for thermally emitted radiation.

Object	Percent
7 sec. disk 3	.08
12 left apt.	1.45
14 right apt.	.55
15 sec. cone 4	.09
17 sec. cone 5	.09
19 sec. cone 1	76.69
20 sec. apt	3.04
21 strut back	.13
25 inner tip end	.09
26 left inner conical	.01
27 middle inner conical	.01
32 secondary mirror	.95
33 primary mirror	10.23
34 sec. cone 6	.07
36 damaged area	2.64
37 sec. cone 7	.07
39 sec. cone 8	.02
41 sec. cone 9	.08
42 sec. disk 9	.33
43 sec. cone 10	3.30
46 stimulator	.07

The table contains no surprises as the mechanisms are similar to scatter from the sunshade. The irradiance on the image for the four infrared wavebands is shown in Table 28.

Table 28. Detector irradiance from thermal emittance

waveband	8-15μ	15-30μ	48-81μ	87-118μ
irradiance w/cm^2	1.82×10^{-19}	1.16×10^{-17}	2.7×10^{-17}	8.02×10^{-18}

The detector area in this case, as in the whole analysis, is 0.0864 cm^2, resulting from a 0.72 x 0.12 cm detector.

Earth integration

The APART earth integration routine was used to determine the irradiance on the detector. Strictly speaking, the results must be considered as an estimate because the routine assumes the telescope is symmetrical about the optical axis. This is not the case because of the sliced off sunshade. The estimation will, however, be on the high side because the A(θ) is lower for out-of-the-meridonal plane source angles. (APART uses the A(θ) for the meridonal plane or the 180° azimuth.)

The earth integration was done for only the angles of 88, 110, and 120 degrees and not the 130° and 150° because the results would be irrelevant at the higher two angles. The reason for this is that the earth, at 130° from the optical axis on the +y side, actually has the other edge at about -50° (sun side of the shade) for which no A(θ) was calculated. This assumes a 180° wide earth at the 900 km

orbital altitude, which is excessive, but the problem of the earth being on both sides of the optical axis remains.

The results of the earth integration are presented in Table 29 for the four infrared wavebands and the three earth limb angles. The earth is considered to be an 288° black body of emissivity 1.0.

Table 29. Detector irradiance due to the earth.

Source Angle	Wavelength 8-15	15-30	48-81	87-118(microns)
88°	1.0×10^{-15}	9.1×10^{-16}	9.1×10^{-16}	9.7×10^{-16}
110°	1.5×10^{-16}	1.2×10^{-16}	1.0×10^{-16}	9.9×10^{-17}
120°	3.6×10^{-19}	3.3×10^{-19}	3.5×10^{-19}	3.7×10^{-19}
	Irradiance in w/cm^2			

Comparison with Previous Analysis

A number of engineering changes have occurred in the IRAS design to improve the stray light rejecting properties. Combined with this change are the measurements of the scattering properties of the primary mirror and also the unfortunate problem of the damaged area on the primary mirror. As a result of these changes, a comparison indicating the effectiveness of the engineering alterations is impossible. Even comparing the results of the two analyses is dubious because pure diffraction is not included in this analysis, and the diffraction scatter mechanism was not calculated for the previous analysis. In spite of these numerous precautions, scientific curiosity prevails with

the result being Figures 18 and 19 for the visible and 11.5 infrared wavelengths. Considering the above mentioned differences, the differences in the two analyses seems small.

7.0 SUMMARY AND CONCLUSION

The analysis of the IRAS optical system for stray light that was presented in this report is not a complete analysis for a number of reasons cited at the beginning of this report. For instance, the omission of pure diffraction from this analysis left out the major contributor at some angles and wavelengths, but this addition would seldom add more than an order of magnitude to the expected result. Similarly, including ten more vane edges as diffracting objects, as was done for one edge in this report, would increase the $A(\theta)$ by at most a factor of 5 in the 8-15μ level; in the 87-118μ level the increase would be the full factor of ten. In spite of these omissions, the analysis indicates that IRAS's $A(\theta)$ is generally below the specification albeit not by much in some cases.

The agreement with the previous analysis also is surprisingly close considering the number of changes made to the system. It appears that the unfortunate damage to the primary mirror and also the worse than expected BRDF of the mirror are in general offset by the improved designs of the secondary baffle. Many of the discrepancies between the two analyses(Figures 18 and 19) are ascribable to the lack of sufficient analysis points in the first analysis.

The conclusion that can be drawn from the thermal emission analysis and the earth integration is that thermal emission does appear to be the major contributor at 120° off axis for the 15 - 30μ, 48 - 81μ, and 87 - 118μ bands. The thermal emission contribution could rise

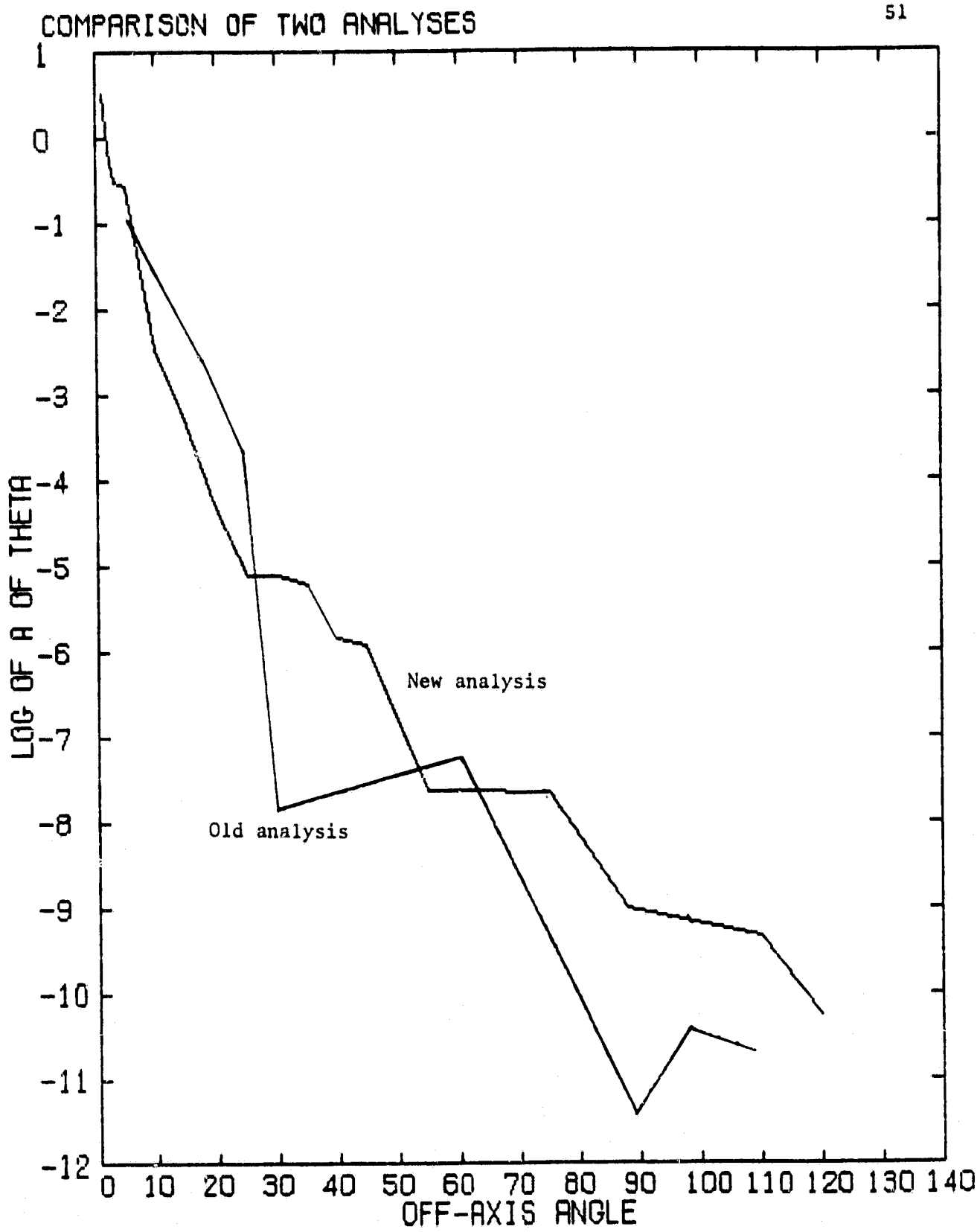

Figure 18. Comparison of analyses - visible.

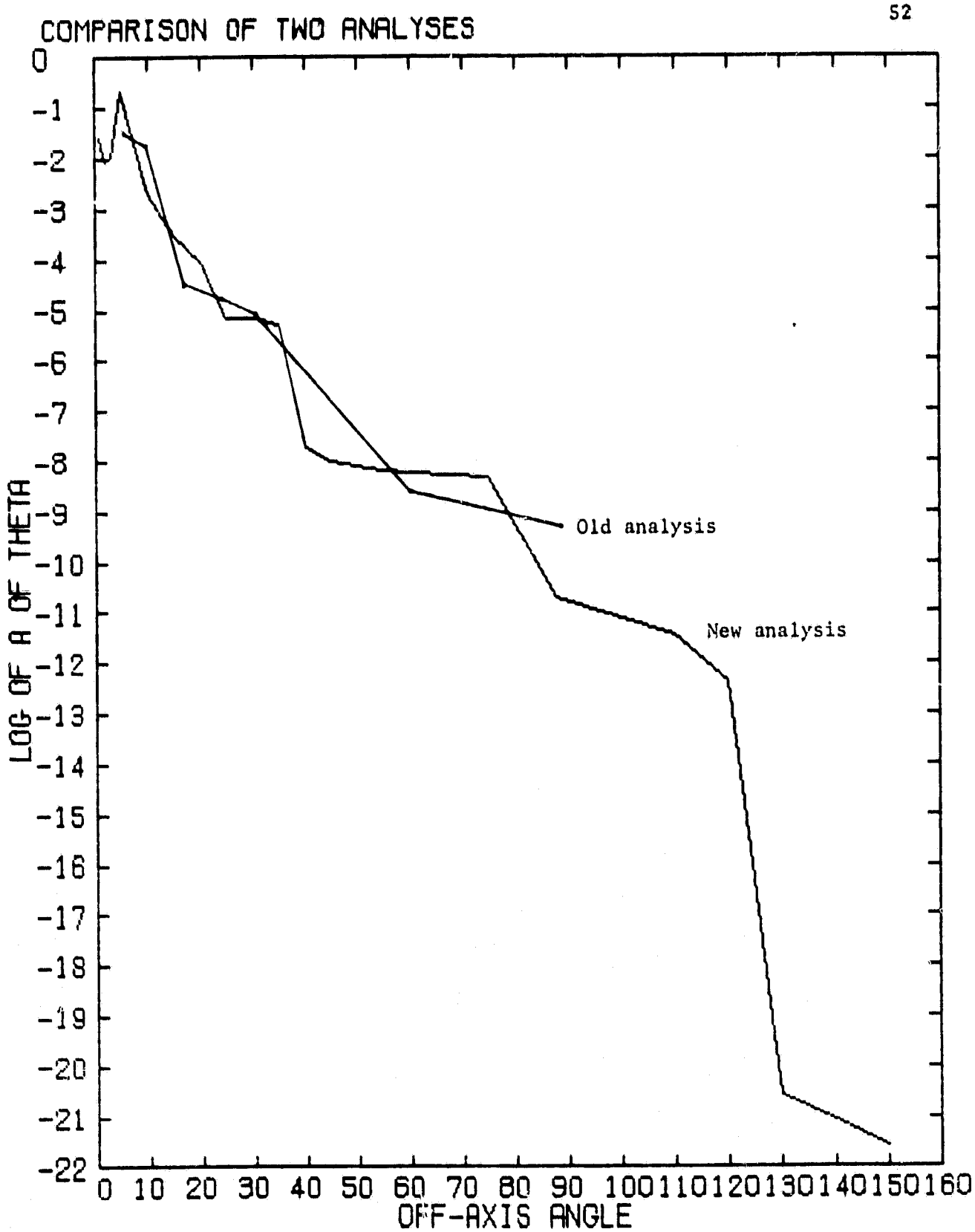

Figure 19. Comparison of analyses - infrared 11.5μm.

if some parts of the interior of IRAS rise above $4^{o}K$.

Finally, there are two suggestions we must make: The first is that the remainder of the analysis be completed to characterize better all of the stray light contributors; this should include the four items discussed on pages 2 and 3, with the addition of a set of point source angles in the sun's direction with respect to the sunshade. This last task would be used to calculate the sun's stray light contribution as well as the earth's contribution for limb angles larger than 120^{o}.

Second, BRDF measurements are desperately needed on all materials and optical components at wavelengths longer than 10.6μ. The measurements should include the full BRDF profile, not just an emissivity measurement, and should extend to at least 120μm.

References

1. Harvey, J. E., Light Scattering Characteristics of Optical Surfaces, Ph. D. Dissertation, University of Arizona (1976).

Appendix A.

INFRARED ASTRONOMICAL SATELLITE (IRAS)

BREAULT RESEARCH ORGANIZATION
1161 El Dorado Place Suite 340
Tucson, Arizona 85715

Assumptions to be used in the Analysis
of the New IRAS Design.

November 22, 1979

Description of the IRAS system as input to APART

The information for the geometry of the system was taken from drawing #693-10000, revision S, dated 3/20/79. In addition, a number of detailed drawings were used to gather numerical data concerning the secondary skirt baffle and the primary cone baffle. The data as entered into Program One are shown in Table 1 where a coordinate set is used with an origin at the primary mirror vertex. The data can be best interpreted when plotted by the computer as in Figure 1. For clarity, the object numbers used to identify the surfaces (baffles, cones, disks, mirrors, etc.),have been eliminated from most of the plot. Also, optical elements are represented as cones between the inner radius and out radius. We will, of course, use the actual curvature in actual calculations. Objects 5 and 6 (the end of the main tube) are represented as cones with a radius equal to the locus of vane tips.

The stimulator behind the secondary mirror is modeled as a short cone through the mirror followed by a cone and a disk. The cone will be used both as an obscuration and as a possible scattering source.

In task 1.4 of the S.O.W. the only diffracting edge will be the end of the main tube. Although diffraction and then scatter mechanisms do occur from all of the vane edges illuminated, they will not be considered in this analysis.

The main tube nearest to the primary mirror was assumed to not have any vanes upon it. Although small sections of vanes do exist to hide rivets, we feel this omission will not alter the predicted results noticeably. Similarly, uncoated rivets are illuminated by the source at the front of the main tube. These, too, for the aforementioned reason, have not been considered.

Orientation of point source scan

Task 1.2 of the S.O.W. indicated the analysis should be done for (1) a scan in the XY plane in the +Y direction, and (2) in the XZ plane in the -Z direction. Because of certain internal characteristics of APART and the left-handed coordinate set used, we have altered the coordinates to include a scan in the meridional plane and a scan orthogonal to it as shown in Figure 2. The orientation of the struts and the damaged area are also illustrated.

Detector location

The analysis will be conducted for an IR detector located on axis. The modeling associated with this detector is described in the IRAS Report by BRO of August 1978, in great detail. The focal plane is rather large and scattering mechanisms will vary for detectors placed over the surface. Thus, the results will be most accurate for the detector on axis. Any variation over the focal plane is not expected to be large because the critical objects are mainly diffuse and that varying the focal plane locations only changes the solid angle by which these objects can transfer power to the parts of the focal plane.

Table 1. Input of IRAS to APART Program One.

```
* AMES CONTRACT FOR FINAL ANALYSIS OF IRAS SYSTEM
* PERKIN ELMER DESIGN NUMBER 693-10000 REVISION S OF 3/20/79
* UNITS ARE CM
* F/1.5 PRIMARY MIRROR SYSTEM
* INDIVIDUAL DETECTOR SIZED IMAGE PLANE
COATING BAFFLES .01
COATING OPTICS .001 -2.
PRINT SHORT
DIFRACT 49 (APERTURE RING) -1 1 -129.77 34.54
ELIPTEDGE 50 (SUNSHADE TIP) -1 1 90.52 106.8 -188.87
ELIPTEDGE 30 (OUTER SUNSHADE) -1 1 99.6 115.9 -188.87
DIFRACT 47 (FRONT APERTURE EDGE) -1 1 -128.0 31.8
CONE 2 -1 5 -128.5 77.18 -243.87 104.14 (OUTER SHIELD)
CONE 5 -1 5 -128.5 32.3 -84.25 32.3 (OUTER MAIN BAFFLE)
CONE 6 -1 4 -84.25 32.3 -48.89 32.3 (MIDDLE MAIN BAFFLE)
CONE 8 -1 5 -48.89 36.43 -13.02 36.43 (INNER MAIN BAFFLE)
DISK 9 (INNER RIGHT END) -1 2 -13.02 30.53 36.43
DISK 12 (LEFT APT.) -1 1 -4.5 30.15 31.75
CONE 22 (OUTER CONITCAL) 1 5 -1.524 9.26 -35.08 6.31
CONE 24 (OUTER CONICAL TIP) 1 1 -35.08 6.2 -39.91 5.73
DISK 23 (OBSCURATION STOP) -1 1 -1.42 10.87 9.26
CONE 43 (SEC. CONE 10) -1 1 -62.47 11.39 -58.48 11.65
DISK 42 (SEC. DISK 9) 1 1 -62.47 10.29 11.39
DISK 40 (SEC. DISK 8) 1 1 -64.09 9.73 10.43
DISK 38 (SEC. DISK 7) 1 1 -65.64 9.19 9.87
DISK 35 (SEC. DISK 6) 1 1 -66.94 8.76 9.30
DISK 18 (SEC. DISK 5) 1 1 -68.08 8.36 8.86
DISK 16 (SEC. DISK 4) 1 1 -69.02 8.03 8.36
CONE 19 (SEC. CONE 1) -1 2 -74.59 7.46 -70.57 7.46
DISK 14 (RIGHT APT.) 1 1 -4.5 30.15 31.75
DISK 36 (DAMAGED AREA) -1 2 -2.62 2.54 0.
STRUTEDGE 21 -1 10 -54.034 10.541 -16. 32.7 1.78 (STRUT BACK)
OPTIC 33 -1 6 0. 30.7 10. (PRIMARY MIRROR)
RD -180.0
CC -1.01185
REPEAT 5 6 8 9 12 22 24 23 43 42 40 38 35 18 16 14 36 21 19
CONE 26 (LEFT INNER CONICAL) -1 2 -35.08 6.09 -39.91 5.66
DISK 25 (INNER TIP END) -1 1 -35.08 5.66 6.09
CONE 27 (MIDDLE INNER CON.) -1 4 -35.08 5.66 -6.93 7.94
CONE 28 (RIGHT INNER CON.) -1 2 -6.93 7.94 -1.32 7.94
CONE 29 (RIGHT INNER C END) -1 2 -1.32 7.94 -.05 5.36
DISK 20 (SEC. APT) 1 1 -74.59 6.02 7.46
DISK 1 (SEC. DISK 1) 1 1 -70.57 7.46 7.65
CONE 3 (SEC. CONE 2) -1 1 -70.57 7.65 -70.14 7.65
DISK 4 (SEC. DISK 2) 1 1 -70.14 7.65 7.82
CONE 7 (SEC. DISK 3) -1 1 -70.14 7.82 -69.63 7.82
DISK 13 (SEC. DISK 3) 1 1 -69.63 7.82 8.03
CONE 15 (SEC. CONE 4) -1 1 -69.63 8.03 -69.02 8.03
CONE 17 (SEC. CONE 5) -1 1 -69.02 8.36 -68.08 8.36
CONE 34 (SEC. CONE 6) -1 1 -68.08 8.86 -66.94 8.76
CONE 37 (SEC. CONE 7) -1 1 -66.94 9.30 -65.64 9.19
CONE 39 (SEC. CONE 8) -1 1 -65.64 9.87 -64.09 9.73
CONE 41 (SEC. CONE 9) -1 1 -64.09 10.43 -62.47 10.29
CONE 44 (SEC. HOLE CONE) -1 1 -74.743 0.8 -75.14 .835
CONE 45 (STIMULATOR CONE) -1 1 -77.000 0.8 -78.4 .80
DISK 46 (STIMULATOR) 1 3 -78.2 1.0 0.
OPTIC 32 1 4 -74.743 6.85 0.8 (SECONDARY MIRROR
RD -36.4833
CC -2.05511
REPEAT 26 27 28 29 20 19 1 3 4 7 13 15 16 17 18 34 35 37 38 39 40 41 42 43
REPEAT 25
DISK 31 -1 1 18.5 .1658 0. (IMAGE)
DISK 48 (DUPLICAT IMAGE) -1 1 18.5 .1658 0.
OBSCUR 11.77
IGNORE 36 47 31
XEQ
```

COATINGS

There are five significant "coatings" that will be used in the analysis: the undamaged mirror BRDF; the damaged mirror BRDF; the sunshade BRDF; the Martin Black coating on the unvaned section of the main baffle, secondary baffle, and the inner conical baffle; and the Martin Black coated vane sections.

The Undamaged Mirror BRDF

The BRDF data, Table 2, was taken from the 3 sets of measured data shown in Figure 3. In Table 3, the data in Table 1 has been converted to log of BRDF vs. log of $(\beta-\beta_o)$. A linear regression fit of the data, site by site, is given in Table 4, along with the fit to the average values of all the sites. We will use this average value as data input as it best represents all the measured data.

The Damaged Mirror BRDF

The data used for the damaged mirror BRDF was taken from Figure 4. It has 3 more sets of measurements than the four shown in Figure 3. Also, the site numbers do not correlate between the two figures. The data is shown in Tables 5 and 6. Table 7 shows the results of the linear regression fit, along with the average value of all seven positions.

Note, however, that for site 1, the coefficient of determination is not very close to 1. This indicates that the data has a very poor fit. It is also the only significant departure. Therefore, this data does not represent the average performance of the damaged area and should be deleted. This was done and the average value of the remaining six sites used to determine the BRDF, as shown in Table 7. The latter will be used in the analysis unless BRO is directed to do otherwise.

The Sunshade scattering characteristics will be the same as used in the original analysis (Section 3). Basically, the specular beam is based on measured data of a model and an assumed diffuse reflectivity of .05 when the specular component is no longer significant.

BRDF of the Primary in the Visible

The BRDF of the Primary mirror, the damaged and undamaged area combined, was taken from Figure 5. The corresponding BRDF values and the linear regression data is shown in Table 8.

The BRDF of the Secondary Mirror

The same values as used in the original analysis will be used for the BRDF of the Secondary Mirror. These values are:

1.75E-3 at $\beta-\beta_o$=.01	Slope = -1.0	λ = 10.6μm
.414 at $\beta-\beta_o$=.01	= -1.0	λ = .6328μm

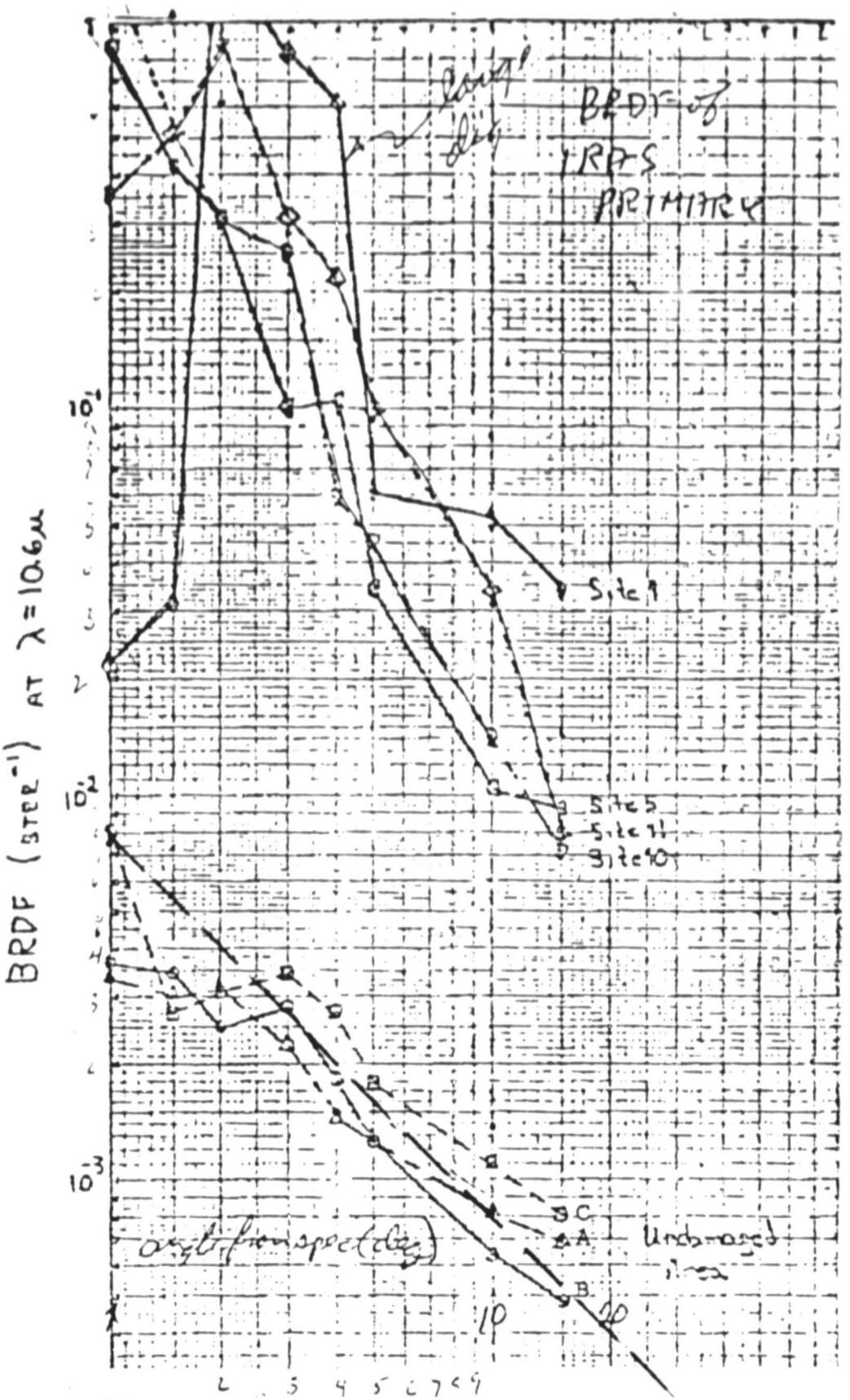

Figure 3 BRDF of the Primary Mirror

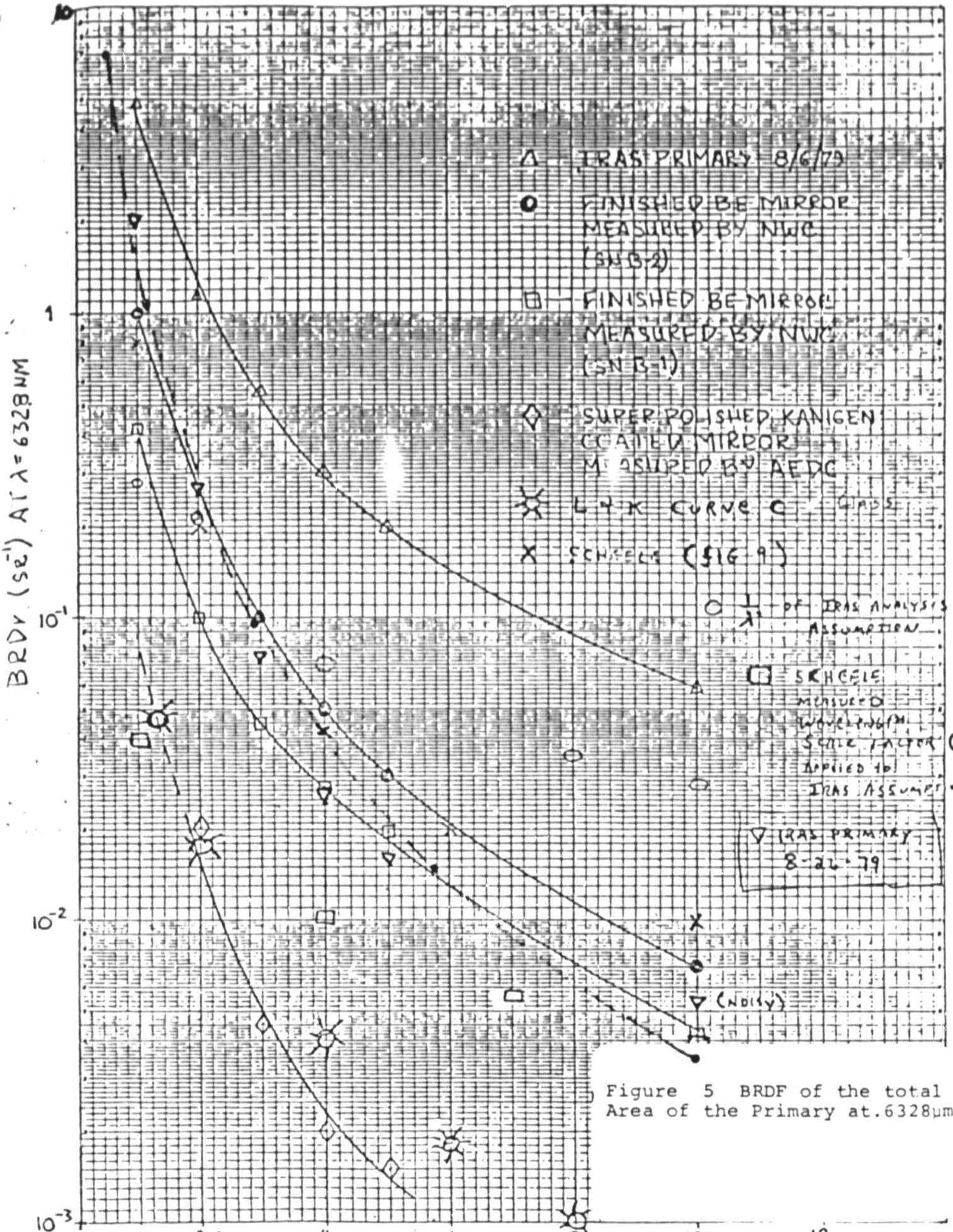

Figure 5 BRDF of the total Area of the Primary at.6328μm

Log BRDF of Undamaged Primary

Site	Degrees From Specular							
	1.0	1.5	2.0	3.0	4.0	5.0	10.0	20.0
A	8.0E-3	2.7E-3	3.1E-3	3.2E-3	2.7E-3	1.8E-3	1.1E-3	8.0E-4
B	3.6E-3	3.5E-3	2.5E-3	2.8E-3	1.8E-3	1.3E-3	4.4E-4	2.9E-4
C	3.5E-3	3.0E-3	3.0E-3	2.2E-3	1.5E-3	1.3E-3	8.2E-4	6.9E-4
AVG	5.0E-3	3.1E-3	2.9E-3	2.8E-3	2.0E-3	1.4E-3	7.9E-4	5.9E-4

TABLE 2 Measured BRDF at Three Different Locations on Undamaged Areas of the primary.

Log BRDF of Undamaged Primary

Site	$\text{Log}(\beta-\beta_0)$							
	.24	.42	.54	.72	.84	.94	1.24	1.53
A	-2.097	-2.569	-2.509	-2.488	-2.581	-2.757	-2.959	-3.097
B	-2.444	-2.456	-2.602	-2.553	-2.745	-2.903	-3.357	-3.538
C	-2.456	-2.523	-2.523	-2.658	-2.824	-2.903	-3.086	-3.161
AVG	-2.298	-2.513	-2.542	-2.561	-2.695	-2.848	-3.102	-3.229

TABLE 3 Log of Measured BRDF versus $\text{Log}(\beta-\beta_0)$

Site	Coefficient of Determination	Log[BRDF(.01)]	Slope (In $\beta-\beta_0$ Space)
A	.878	-2.085	-.677
B	.924	-2.069	-.935
C	.959	-2.268	-.616
AVG	.967	-2.135	-.727

TABLE 4 Linear Regression Fit of Log(BRDF) versus $\text{Log}(\beta-\beta_0)$

Degrees From Specular	BRDF by Site								
	AVG6	5	3	8	10	11	1	9	AVG7
1.0	1.527	.85	3.0	2.0	1.7	.36	.022	1.25	1.31
1.5	1.027	.42	2.4	1.55	.5	.51	.033	.78	.88
2.0	.608	.32	.9	.55	.89	.31	2.4	.68	.86
3.0	.276	.1	.65	.12	.32	.25	.85	.215	.36
4.0	.094	.1	.18	.064	.12	.058	.6	.042	.24
5.0	.091	.034	.24		.1	.046	.06	.034	.14
10.0	.031	.01	.085	.03	.035	.014	.053	.0135	.052
20.0	.014	.0092	.031	.0122	.008	.007	.035	.018	.045

TABLE 5 Measured BRDF of Seven Different Locations Along the Damaged Area.

DEGREES From Specular	Log($\beta-\beta_0$)	Log of BRDF by Site AVG6	5	3	8	10	11	1	9	AVG7
1.0	-1.76	.184	-.071	.477	.301	.23	-.444	-1.658	.097	.117
1.5	-1.58	.011	-.377	.38	.190	-.301	-.292	-1.481	-.108	-.056
2.0	-1.46	-.216	-.495	-.046	-.26	-.051	-.509	.38	-.167	-.066
3.0	-1.28	-.559	-1.000	-.187	-.921	-.495	-.602	-.071	-.668	-.444
4.0	-1.16	-1.027	-1.000	-.745	-1.194	-.921	-1.237	-.222	-1.377	-.620
5.0	-1.06	-1.042	-1.469	-.620		-1.000	-1.337	-1.222	-1.469	-.854
10.0	-0.76	-1.505	-2.000	-1.071	-1.523	-1.456	-1.854	-1.276	-1.87	-1.284
20.0	-0.47	-1.847	-2.036	-1.509	-1.914	-2.097	-2.155	-1.456	-1.745	-1.347

TABLE 6 Log of Measured BRDF of Seven Different Damage Locations.

Site	Coefficient of Determination	Log[BRDF(.01)]	Slope (In $\beta-\beta_0$ Space)
5	.95	.30	-1.678
3	.96	.88	-1.60
8	.93	.66	-1.80
10	.97	.67	-1.76
11	.93	.22	-1.573
1	.02	-.66	-0.270
9	.86	.48	-1.728
AVG7	.96	.47	-1.286
AVG6	.98	.61	-1.682

TABLE 7 Linear Regression Fit of Log(BRDF) versus Log($\beta-\beta_0$)

BRDF of the Primary at .6328μm

Angle of Incidence	Log$(\beta-\beta_0)$	Log(BRDF)	BRDF
1.	-1.758	.301	2.0
2	-1.457	-.569	.27
3	-1.281	-1.125	.075
4	-1.156	-1.585	.026
5	-1.06	-1.796	.016
10	-0.760	-2.268	.0054

Coefficient of Determination	Log(BRDF(.01))	SLOPE
.976	.844	-2.674

TABLE 8 BRDF of the Primary in the Visible

Martin Black

The same internal model of Martin Black will be used as in the original analysis. Its BRDF is depicted in Figure A10 (reproduced herein).

Main Baffle with Vanes

The forward section of vanes have:

(1) A 90° vane angle (i.e., vertical)
(2) Vanes 8.85 cm apart
(3) Vanes 4.42 cm deep
(4) A .01 diffuse coating
(5) An aperture radius of 32. cm
(6) An edge radius on the vane edge of .01 cm

The center portion of the main baffle also has vanes on it, but the vane spacing is 4.42 cm.

Thermal Emittance

The Sunshade temperature is assumed to be 80° K (nominal). The emissivity is assumed to be $\epsilon = .02$ from which other values can easily be scaled.

SUMMARY

These are all the pertinent assumptions that come to light in setting up the analysis. If other assumed values are desired please contact me as soon as possible.

Sincerely,

Robert Breault,
BREAULT RESEARCH ORGANIZATION, INC.

/j

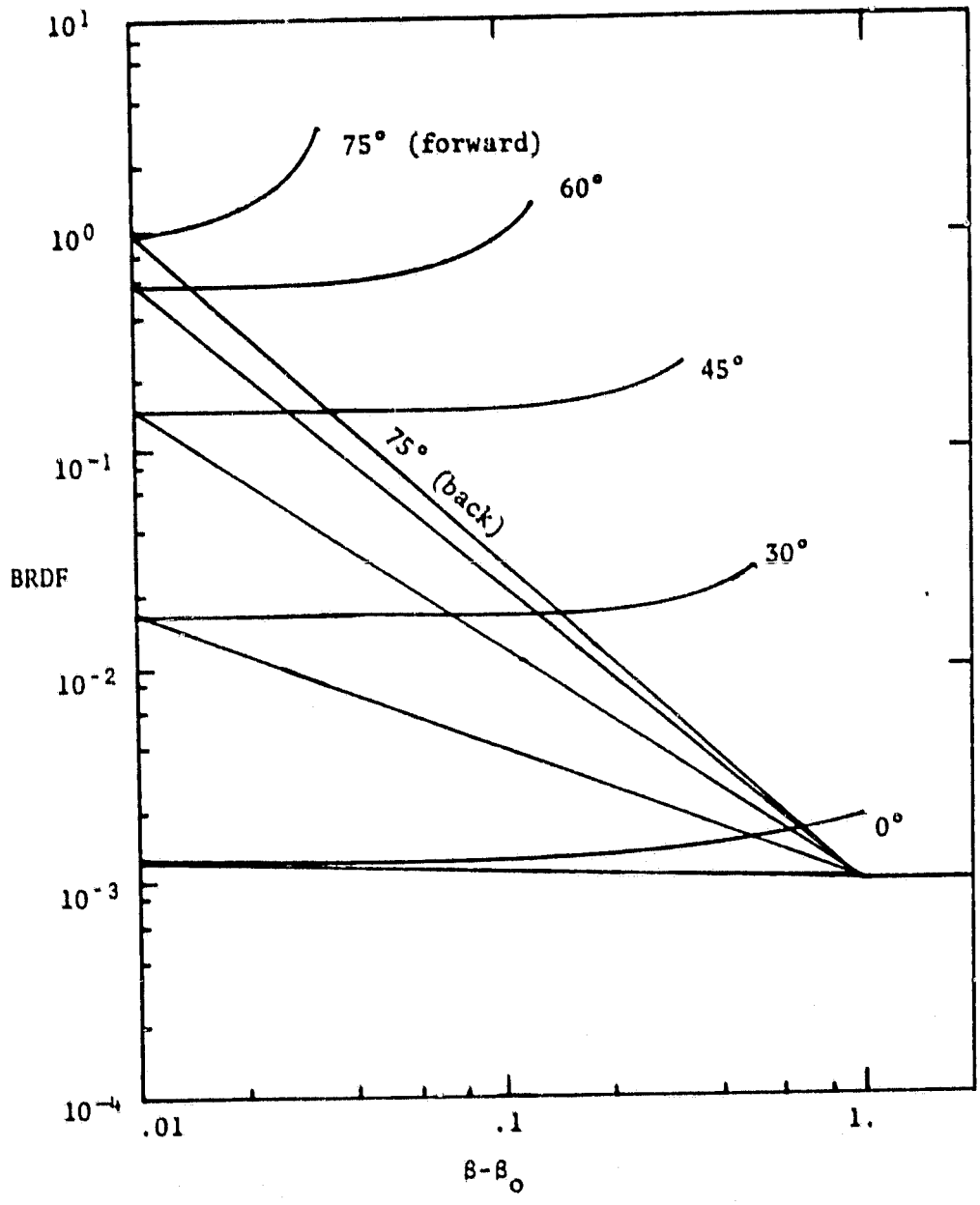

Fig. A10. BRDF of Martin Black Model.